

THE BOUNDARY METHOD FOR SEMI-DISCRETE OPTIMAL TRANSPORT PARTITIONS AND WASSERSTEIN DISTANCE COMPUTATION

LUCA DIECI AND J.D. WALSH III

ABSTRACT. We introduce a new technique, which we call the *boundary method*, for solving the semi-discrete optimal transport problem, a special, but quite general, type of optimal transportation. We provide mathematical justification, convergence analysis, algorithmic development, and testing.

1. INTRODUCTION

In this work, we consider a new solution method for optimal transport problems. Numerical optimal transport has applications in a wide range of fields, but the scaling properties and ground cost restrictions of current numerical methods make it difficult to find solutions for many applications.

Key challenges in numerical optimal transport are: (a) the design of numerical methods capable of handling general ground costs (b) efficient computation of the Wasserstein metric, and (c) solutions of three (or higher) dimensional problems. We propose the boundary method below to address these concerns for a broad class of optimal transportation problems: *semi-discrete transport*. Semi-discrete formulations can be used to approximate solutions to fully continuous problems, and the semi-discrete optimal transport problem is of practical relevance itself.

1.1. Description of optimal transport: the Monge-Kantorovich problem. The theory of optimal transport dates back to the work by Monge in 1781, [20]. In the 1940s, Kantorovich's papers [15, 16] relaxed Monge's requirement that no mass be split, creating we now know as the Monge-Kantorovich problem.

Definition 1.1 (Monge-Kantorovich problem). Let $X, Y \subseteq \mathbb{R}^d$, let μ and ν be probability densities defined on X and Y , and let $c(\mathbf{x}, \mathbf{y}) : X \times Y \rightarrow \mathbb{R}$ be a measurable *ground cost* function. Define the set of *transport plans*

$$\Pi(\mu, \nu) := \left\{ \pi \in \mathcal{P}(X \times Y) \mid \begin{array}{l} \pi[A \times Y] = \mu[A], \pi[X \times B] = \nu[B], \\ \forall \text{ meas. } A \subseteq X, B \subseteq Y \end{array} \right\}, \quad (1.1)$$

where $\mathcal{P}(X \times Y)$ is the set of probability measures on the product space, and define the *primal cost* function $P : \Pi(\mu, \nu) \rightarrow \mathbb{R}$ as

$$P(\pi) := \int_{X \times Y} c(\mathbf{x}, \mathbf{y}) d\pi(\mathbf{x}, \mathbf{y}). \quad (1.2)$$

The Monge-Kantorovich problem is to find the *optimal primal cost*

$$P^* := \inf_{\pi \in \Pi(\mu, \nu)} P(\pi), \quad (1.3)$$

and an associated *optimal transport plan*

$$\pi^* := \arg \inf_{\pi \in \Pi(\mu, \nu)} P(\pi). \quad (1.4)$$

Kantorovich also identified the problem's dual formulation.

1991 *Mathematics Subject Classification*. 65K10 and 90C08 and 49M25.

Key words and phrases. Optimal transport and Monge-Kantorovich and semi-discrete and Wasserstein distance and boundary method.

Acknowledgments. This material is based upon work supported by the National Science Foundation Graduate Research Fellowship Program under Grant No. DGE-1650044. Any opinions, findings, and conclusions or recommendations expressed in this material are those of the authors and do not necessarily reflect the views of the National Science Foundation.

Definition 1.2 (Dual formulation). Define the set of functions

$$\Phi_c(\mu, \nu) := \left\{ (\varphi, \psi) \in L^1(d\mu) \times L^1(d\nu) \mid \begin{array}{l} \varphi(\mathbf{x}) + \psi(\mathbf{y}) \leq c(\mathbf{x}, \mathbf{y}), \\ d\mu \text{ a.e. } \mathbf{x} \in X, d\nu \text{ a.e. } \mathbf{y} \in Y \end{array} \right\}. \quad (1.5)$$

Let the *dual cost function*, $D : \Phi_c(\mu, \nu) \rightarrow \mathbb{R}$, be defined as

$$D(\varphi, \psi) := \int_X \varphi d\mu + \int_Y \psi d\nu. \quad (1.6)$$

Then, the *optimal dual cost* is

$$D^* := \sup_{(\varphi, \psi) \in \Phi_c(\mu, \nu)} D(\varphi, \psi), \quad (1.7)$$

and an optimal dual pair is given by

$$(\varphi^*, \psi^*) := \arg \sup_{(\varphi, \psi) \in \Phi_c(\mu, \nu)} D(\varphi, \psi). \quad (1.8)$$

For a given ground cost function c , Monge-Kantorovich solutions are related to the *Wasserstein metric*, a distance between probability distributions:

$$W_p(\mu, \nu) := \inf_{\pi \in \Pi(\mu, \nu)} \left(\int_{X \times Y} c(\mathbf{x}, \mathbf{y})^p d\pi(\mathbf{x}, \mathbf{y}) \right)^{1/p}. \quad (1.9)$$

We have $W_1(\mu, \nu) = P^* = D^*$, and hence, we may refer to any of these as the *Wasserstein distance*, the *optimal transport cost*, or simply the *optimal cost*.

Remark 1.3. $W_p(\mu, \nu)$ is often written as W_p , with μ and ν implied. Furthermore, as Equation (1.9) makes clear, $W_p(\mu, \nu)$ always depends on the ground cost function $c(\mathbf{x}, \mathbf{y})$. In the literature, W_1 is sometimes used as a default notation when the ground cost is given by the Euclidean distance $\|\mathbf{x} - \mathbf{y}\|_2$ (e.g., see [18]), and W_2^2 is occasionally used to indicate that the ground cost is the squared- ℓ_2 distance $\|\mathbf{x} - \mathbf{y}\|_2^2$.

Definition 1.4 (Monge problem). In certain cases, there exists at least one solution to the semi-discrete Monge-Kantorovich problem that does not split transported masses. In other words, there exists some π^* such that

$$\pi^*(\mathbf{x}, \mathbf{y}) = \pi_{T^*}^*(\mathbf{x}, \mathbf{y}) := \mu(\mathbf{x}) \delta[\mathbf{y} = T^*(\mathbf{x})], \quad (1.10)$$

where $T^* : X \rightarrow Y$ is a measurable map called the *optimal transport map*. When such a π^* exists, we say the solution also solves the Monge problem.

If the Monge problem has a solution, we can assume without loss of generality that every $\pi \in \Pi(\mu, \nu)$ satisfies

$$\pi(\mathbf{x}, \mathbf{y}) = \pi_T(\mathbf{x}, \mathbf{y}) := \mu(\mathbf{x}) \delta[\mathbf{y} = T(\mathbf{x})], \quad (1.11)$$

for some measurable transport map $T : X \rightarrow Y$, and that the primal cost can be written

$$P(\pi) := \int_X c(\mathbf{x}, T(\mathbf{x})) d\mu(\mathbf{x}). \quad (1.12)$$

1.2. Numerical approaches to the MK problem. Applications of optimal transport are found in many areas of research, including medicine, economics, image processing, machine learning, physics, and many others; e.g., see [21, 7, 13, 9, 6]. For that reason, many people have focused their research on numerical approximation of the Monge-Kantorovich problem.

The current approaches can be broadly separated into two classes: (1) discrete methods, which ignore the continuity implicit in the product space, and (2) continuous methods, which use the continuity of the product space to speed computation.

Discrete methods fully discretize both (X, μ) and (Y, ν) , and solve the resulting minimization problem using network flow minimization techniques. As described in [17], there are over 20 established methods for solving such problems, and at least seven software packages capable of handling one or more of these methods.

More recent development has focused on continuous methods. The Monge-Kantorovich dual problem can be reformulated as a Monge-Ampère-type partial differential equation:

$$-\nabla \cdot (a \nabla u) = f, \text{ where } |\nabla u| \leq 1, a \geq 0, \text{ and } |\nabla u| < 1 \implies a = 0. \quad (1.13)$$

If the ground cost function is strictly convex, or satisfies the regularity conditions described in [19], the problem is well-posed. To date, this has largely restricted the application of continuous methods to well-behaved cost functions such as a squared or regularized Euclidean distance. Continuous methods currently in use apply finite difference, gradient descent, or Bregman's method, all attempting to map X to a fully discretized Y [11, 14, 2].

In both approaches, the problem is fully discretized, and the complexity of the approach is relative to the size of the discretization. For purposes of evaluating complexity, assume we discretize X into W^d elements, and Y into N elements. The resulting network has $W^d + N \sim \mathcal{O}(W^d)$ nodes and $W^d N$ arcs.

Discrete approaches have been applied to optimal transport since the mid-20th century, and most have well-understood complexity bounds. The minimum cost flow approaches described in [17] all have complexity $\mathcal{O}(W^{2d}N)$ or worse; e.g., see [22]. Continuous approaches focus less on complexity analysis, but a typical claim is the $\mathcal{O}(W^{2d})$ (i.e., quadratic) complexity described in [9].

1.3. Semi-discrete problem. The semi-discrete optimal transport problem is the Monge-Kantorovich problem of Definition 1.1, with restrictions on μ and ν , and c :

- (1) Assume that μ satisfies the following:
 - (a) μ is bounded.
 - (b) μ is nonatomic.
 - (c) μ is continuous except on a set of Lebesgue measure zero.
 - (d) The support of μ is contained in the convex compact region $A \subseteq X$.
- (2) Assume ν has exactly $n \geq 2$ non-zero values, located at $\{\mathbf{y}_i\}_{i=1}^n \subseteq Y$.
- (3) Assume c is an admissible ground cost function, as described in Definition 1.6.

Remark 1.5. We assume $n \geq 2$ because if $n = 1$ the optimal transport solution is trivial: $T(\mathbf{x}) \equiv \mathbf{y}_1$ for all $\mathbf{x} \in X$, and

$$P^* = \nu(\mathbf{y}_1) \int_A c(\mathbf{x}, \mathbf{y}_1) d\mu(\mathbf{x}) = \int_A c(\mathbf{x}, \mathbf{y}_1) d\mu(\mathbf{x}). \quad (1.14)$$

Definition 1.6 (Admissible ground cost). An *admissible ground cost* function is a measurable, continuous, function $c(\mathbf{x}_1, \mathbf{x}_2) : \mathbb{R}^d \times \mathbb{R}^d \rightarrow \mathbb{R}$, satisfying the following properties:

- (1) $c(\mathbf{x}, \mathbf{x}) = 0$ for all $\mathbf{x} \in \mathbb{R}^d$;
- (2) $c(\mathbf{x}_1, \mathbf{x}_2) = c(\mathbf{x}_2, \mathbf{x}_1) > 0$ for all $\mathbf{x}_1, \mathbf{x}_2 \in \mathbb{R}^d$ such that $\mathbf{x}_1 \neq \mathbf{x}_2$;
- (3) for any collinear points $\mathbf{x}_1, \mathbf{x}_2, \mathbf{x}_3 \in \mathbb{R}^d$, $\|\mathbf{x}_1 - \mathbf{x}_2\|_2 \leq \|\mathbf{x}_3 - \mathbf{x}_2\|_2$ implies $c(\mathbf{x}_2, \mathbf{x}_1) \leq c(\mathbf{x}_2, \mathbf{x}_3)$.

Remark 1.7. Examples of admissible ground cost functions:

- (a) If c is an ℓ_p function, $p > 0$, then c is an admissible ground cost function.
- (b) If c is an admissible ground cost function and $\tilde{c} = c^q$ for some $q > 0$, then \tilde{c} is an admissible ground cost function.
- (c) If $\{c_i\}_{i=1}^m$ is a set of admissible ground cost functions, and c be a linear combination of $\{c_i\}_{i=1}^m$ with positive coefficients,

$$c := \sum_{i=1}^m k_i c_i \quad \text{s.t. } k_i > 0 \quad \forall i \in \mathbb{N}_m, \quad (1.15)$$

then c is an admissible ground cost function.

These results can be obtained by elementary algebraic manipulation.

For all c and all $\mathbf{x} \in \mathbb{R}^d$, $S \subseteq \mathbb{R}^d$, we define

$$c(\mathbf{x}, S) := \inf_{\mathbf{s} \in S} c(\mathbf{x}, \mathbf{s}). \quad (1.16)$$

Remark 1.8. The semi-discrete problem has interesting applications in its own right. Recent developments include work on the semi-discrete principal-agent problem and systems of unequal dimension; see [10, 8]. There are also obvious similarities between the semi-discrete problem and (generalized) Voronoi diagrams, similarities that are clearly recognized in [25]. These similarities notwithstanding, the semi-discrete optimal transportation problem is considerably more general, and our numerical method departs from any used in the context of Voronoi tessellations.

1.3.1. *Semi-discrete transport and the Monge problem.* Because c is continuous and μ is nonatomic, at least one solution to the semi-discrete Monge-Kantorovich problem also satisfies the Monge problem, described in Definition 1.4; see [23]. Thus, by applying Equation (1.11), we can assume without loss of generality that any transport plan π partitions A into n sets A_i , where A_i is the set of points in A that are transported by the map T to \mathbf{y}_i . Using this partitioning scheme in combination with Equation (1.12) allows us to rewrite the primal cost function for the semi-discrete problem as

$$P(\pi) := \sum_{i=1}^n \int_{A_i} c(\mathbf{x}, \mathbf{y}_i) d\mu(\mathbf{x}). \quad (1.17)$$

1.4. **Shift characterization for semi-discrete optimal transport.** Using this idea of sets A_i , we are ready to describe the shift characterization of the semi-discrete optimal transport problem. For this, we follow the very clear exposition of Rachev, Rüschendorf, and Uckelmann (see [23, 24, 25]).

Definition 1.9 (Shift characterization). Let $\{a_i\}_{i=1}^n$ be a set of n finite values, referred to as *shifts*. Define

$$F(\mathbf{x}) := \max_{1 \leq i \leq n} \{a_i - c(\mathbf{x}, \mathbf{y}_i)\}. \quad (1.18)$$

For $i \in \mathbb{N}_n$, where $\mathbb{N}_n = \{1, \dots, n\}$, let

$$A_i := \{\mathbf{x} \in A \mid F(\mathbf{x}) = a_i - c(\mathbf{x}, \mathbf{y}_i)\}. \quad (1.19)$$

Note that $\cup_{i=1}^n A_i = A$. The problem of determining an optimal transport plan π^* is equivalent to determining shifts $\{a_i\}_{i=1}^n$ such that for all $i \in \mathbb{N}_n$, $\mu(A_i) = \nu(\mathbf{y}_i)$.

Remark 1.10. The shift characterization has seen some application in the literature of numerical optimal transport. Of particular note for us is the work [25], where Rüschendorf and Uckelmann report on some numerical experiments relative to costs given by ℓ_2^2 and ℓ_p functions with $p = 2, 3, 4, 10$. They assume that μ is the uniform distribution, and test various weights and placements for the set $\{\mathbf{y}_i\}_{i=1}^n$. When an exact solution cannot be directly determined, they fully discretize the problem and use a linear programming solver. Rüschendorf and Uckelmann are well aware of the large computational expense of this approach, which may explain why they restrict approximation of solutions to one-dimensional distributions and problems in \mathbb{R}^2 with relatively few \mathbf{y}_i 's ($n \leq 15$). In [25], Rüschendorf and Uckelmann do not discuss approximating the Wasserstein distance, even for problems where an exact optimal transport map is known.

The shift characterization is also discussed in [1].¹ This paper of Barrett and Prigozhin proposes a new numerical method for the optimal transport problem with ground cost given by the Euclidean distance. Starting with an alternative form of Equation (1.13), taken from [5], Barrett and Prigozhin develop a mixed formulation of the Monge-Kantorovich problem, which they solve using a standard finite element discretization. In the numerical examples, a single set of five \mathbf{y}_i 's is given, solved exactly with $a_i \equiv 0$ for all i , and then approximated with μ and ν both uniform distributions (continuous and discrete, respectively). Aside from the complexity of Barrett and Prigozhin's approach, including the difficulties inherent in the mesh selection process and the sensitive limiting process in the regularization parameter, they are not able to adequately resolve the region boundaries, which are at best blurred; see [1, Figure 3]. Like Rüschendorf and Uckelmann, Barrett and Prigozhin's paper does not concern itself with the Wasserstein distance.

2. BOUNDARY METHOD

Here, we introduce our new method: the *boundary method*. At a high level, the idea of the method is simple: track only the boundaries between regions, without resolving the regions' interiors. To do this in practice and obtain an efficient technique, we must account for the interplay between discretization, a mechanism for discarding interior regions, and a fast solver.

¹In [1], the shift characterization is called an "optimal coupling."

2.1. Boundary identity and system of equations. For all $i, j \in \mathbb{N}_n$ such that $i \neq j$, let

$$A_{ij} := A_i \cap A_j. \quad (2.1)$$

The *boundary set* is defined as

$$B := \bigcup_{1 \leq i < n} \bigcup_{i < j \leq n} A_{ij}, \quad (2.2)$$

and for each $i \in \mathbb{N}_n$, let the *strict interior* of A_i be defined as

$$\mathring{A}_i := A_i \setminus B. \quad (2.3)$$

For all $i, j \in \mathbb{N}_n$ such that $i \neq j$, define $g_{ij} : X \rightarrow \mathbb{R}$ as

$$g_{ij}(\mathbf{x}) := c(\mathbf{x}, \mathbf{y}_i) - c(\mathbf{x}, \mathbf{y}_j). \quad (2.4)$$

By Corollary 3.10 below, $B \neq \emptyset$ and for each $\mathbf{x} \in B$ there exist $i, j \in \mathbb{N}_n$, $i \neq j$, such that $\mathbf{x} \in A_{ij}$. Because $\mathbf{x} \in A_i$, we have $F(\mathbf{x}) = a_i - c(\mathbf{x}, \mathbf{y}_i)$, and because $\mathbf{x} \in A_j$, we have $F(\mathbf{x}) = a_j - c(\mathbf{x}, \mathbf{y}_j)$. Combining and rearranging these, we get

$$g_{ij}(\mathbf{x}) = a_i - a_j, \quad \forall \mathbf{x} \in A_{ij}. \quad (2.5)$$

Thus, Equation (2.5) implies that A_{ij} is a subset of a level set of g_{ij} ; the value $a_i - a_j$ is constant, regardless of which $\mathbf{x} \in A_{ij}$ is chosen. Using this information, for each $i, j \in \mathbb{N}_n$, $i \neq j$, such that $A_{ij} \neq \emptyset$, we can define the constant *shift difference*

$$a_{ij} := g_{ij}(\mathbf{x}_{ij}) \quad \forall \mathbf{x}_{ij} \in A_{ij}. \quad (2.6)$$

Given a sufficiently large set of functionally independent equations of the form given in Equation (2.6), one could determine most or all of the shifts $\{a_i\}_{i=1}^n$. As we show in Theorem 3.12, it is possible to obtain exactly $(n - 1)$ functionally independent equations of the desired form, but a set of n such independent equations does not exist.

Since we know that the set of shifts allows exactly one degree of freedom, the boundary method's approach is to obtain $(n - 1)$ well-chosen a_{ij} values, fix one a_i , and use functionally independent equations of the form (2.6) to solve for the remaining $(n - 1)$ shifts. The crucial observation is that for the a_i 's, there is no need to retain information about interior of the regions.

The Wasserstein distance can also be computed without saving region interiors. Once we have determined that $R \subset A_i$ for some region R , the (partial) Wasserstein distance corresponding to R is equal to

$$P_R := \nu(\mathbf{y}_i) \int_R c(\mathbf{x}, \mathbf{y}_i) d\mu(\mathbf{x}), \quad (2.7)$$

and the total Wasserstein distance P^* is equal to the sum of all such partial distances P_R , computed over every A_i .

Recognizing these facts, inherent in the shift characterization, inspired both the boundary method's name and its guiding principles, summarized below:

Do *not* approximate the entire transport plan over A ; rather, identify approximate region boundaries and determine $(n - 1)$ shift differences a_{ij} .

2.2. The boundary method. As described below, the boundary method generates a grid A^r approximating the unevaluated region of A , and uses it to determine the subgrid B^r containing the boundary set B . This subgrid is determined by approximating an optimal transport solution from the grid A^r to the point set $\{\mathbf{y}_i\}_{i=1}^n$.

Although not strictly necessary, we will restrict ourselves to $A = [0, l]^d$ and apply a Cartesian grid over that region. At the r -th refinement level of the algorithm, the grid will thus consist of a collection of boxes with width w_r in each dimension of our discretization. By a slight abuse of notation, we use \mathbf{x}^r to refer to such a box, centered at the point \mathbf{x} . Thus, $\mu(\mathbf{x}^r)$ refers to the μ -measure of the box of width w_r centered at \mathbf{x} .

Neighboring boxes are those with center points that differ by no more than one unit in any discretization index. The set of *neighbors* of \mathbf{x} is denoted $N(\mathbf{x})$ (defined in Equation (3.8), below). Because regions of μ -measure zero need not be transported to any particular \mathbf{y}_i , boxes of positive weight that are adjacent to such regions are always retained. We refer to such a box as an *edge box*. Thus, the set of edge boxes is

$$\text{edg}(A^r) := \{\mathbf{x} \in A^r \mid \mu(\mathbf{x}) > 0 \text{ and } \mu(\mathbf{x}_n) = 0 \text{ for some } \mathbf{x}_n \in N(\mathbf{x})\}. \quad (2.8)$$

Boundary method algorithm

- (0) Set $\tilde{P} = 0$, $\tilde{\nu} = \nu$, and $r = 1$. Create $A^r = A^1$ from A .
- (1) **Quickly approximate** the discretized transport solution.
- (2) For each $\mathbf{x} \in \text{int}(A^r)$:
 - Are the neighbors of \mathbf{x} all transported to the same \mathbf{y}_i ?
 - If so, then \mathbf{x}^r is in the interior of A_i :
 - [optional] Add $\int_{\mathbf{x}^r} c(\mathbf{z}, \mathbf{y}_i) d\mu(\mathbf{z})$ to \tilde{P} .
 - Reduce the value of $\tilde{\nu}(\mathbf{y}_i)$ by $\mu(\mathbf{x}^r)$.
 - Remove \mathbf{x} from $\text{int}(A^r)$.

The sets $\text{edge}(A^r)$ and the reduced set $\text{int}(A^r)$ combine to form B^r .

- (3) Is the desired refinement reached?
 - If not:
 - Refine B^r to create A^{r+1} , increment r , and go to Step (1).

Once the desired refinement level is reached:

- (4) Use B^r to identify $(n - 1)$ appropriate shift differences $\{a_{ij}\}$ and solve for the shifts $\{a_i\}_{i=1}^n$.
- (5) [optional] Use \tilde{P} and B^r to approximate $W_1(\mu, \nu)$.

Because A contains the support of μ , every box (of positive mass) that is adjacent to the boundary of A is an edge box.

A box whose neighbors and itself all have positive measure is referred to as an *internal box*. The set of internal boxes is

$$\text{int}(A^r) := \{\mathbf{x} \in A^r \mid \mu(\mathbf{x}) > 0 \text{ and } \mu(\mathbf{x}_n) > 0 \text{ for all } \mathbf{x}_n \in N(\mathbf{x})\}. \quad (2.9)$$

Boxes of μ -measure zero are not part of $\text{edge}(A^r)$ or $\text{int}(A^r)$ and they are discarded when the optimal transport problem is solved. We need not be concerned about losing a region A_i due to this discard process, since this would imply $\mu(A_i) = 0$ (and hence $\nu(\mathbf{y}_i) = 0$, which is not possible).

Region interiors are identified by comparing the destination of each $\mathbf{x} \in \text{int}(A^r)$ to the destinations of its neighbors. Edge boxes are never considered part of a region interior, so they are passed directly to B^r .

In order to remove identified region interiors, we also maintain a running total of the untransported mass, given by *partial measure* $\tilde{\nu}$. To preserve the balance of the transport problem, each time a region \mathbf{x}^r is transported from A to \mathbf{y}_i , the remaining amount that can be transported to \mathbf{y}_i , $\tilde{\nu}(\mathbf{y}_i)$, must be reduced by $\mu(\mathbf{x}^r)$.

We can approximate the Wasserstein distance P^* by generating a running total over region interiors: \tilde{P} . This \tilde{P} is an increasing function of r , and for all r , $P^* \geq \tilde{P}$. The Wasserstein distance over any remaining boundary region is evaluated at completion.

Remark 2.1. Further approximations may be required for a truly general algorithm. Depending on μ , it may be necessary to approximate the mass of each box, $\mu(\mathbf{x}^r)$. Depending on μ and c , the Wasserstein distance over each box, given by $\int_{\mathbf{x}^r} c(\mathbf{z}, \mathbf{y}_i) d\mu(\mathbf{z})$, may also require approximation. However, in this work we assume that the integrals can be computed exactly. In practice, this is not a significant limitation. Most numerical applications focus on the exactly-computable cases where μ is uniform and c is either ℓ_2 or ℓ_2^2 . Furthermore, as we show in Section 4, the set of exactly-computable options is quite large.

To illustrate the iterative portion of the boundary method, Steps (1) and (2), we present the following example.

Example 2.2. Let $X = Y = [0, 1]^2$. Assume μ is the uniform probability density, so for all measurable sets $S \subseteq A$, $\mu(S) = |S|$, and that ν has uniform discrete probability density, so $\nu(y_i) = 1/n$ for $1 \leq i \leq n$. Take $n = 5$, with the five points where ν has nonzero density distributed as shown in Figure 1.

Let c be the squared Euclidean norm, $\|\mathbf{y} - \mathbf{x}\|_2^2$. Suppose a discretization with width 2^{-5} is sufficient to provide the desired accuracy and that we apply the boundary method with initial width 2^{-4} .

Figure 1 shows the state of the boundary method during the first iteration. In Figure 1(a), we have just completed Step (1): the approximate transport map has been computed, but we have not identified interior

points or added anything to the partial transport cost \tilde{P} . Figure 1(b) shows the state of the algorithm after Step (2): the interior regions have been identified (shown in gray), and the partial transport cost has been computed for those regions, giving us $\tilde{P} = 0.01387$.

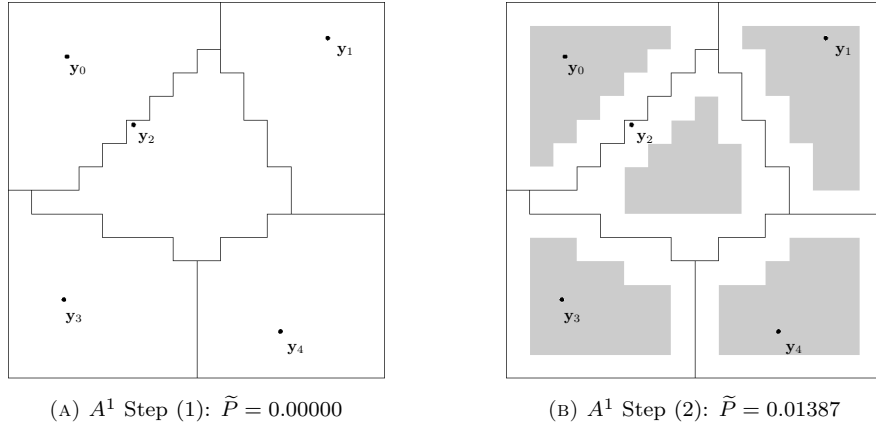


FIGURE 1. Iteration A^1 of Example 2.2 illustrated: $w_1 = 2^{-4}$

Figure 2 shows the state of the boundary method algorithm during the second iteration. In Figure 2(a), Step (1) has just been completed. As can be seen by comparing Figure 1(b) to Figure 2(a), the boundary and interior regions are the same ones that we had at the end of the first iteration, but refining the boundary set to width $w_2 = 2^{-5}$ allows us to compute a more refined transport map. Because Step (1) does not add to the identified interior regions, the partial Wasserstein distance \tilde{P} is also unchanged from Figure 1(b).

After Step (2) of the second iteration, shown in Figure 2(b), more of the interiors have been identified. The partial transport cost shows a corresponding increase: we now have $\tilde{P} = 0.02898$. Because we have achieved our desired refinement, a width of 2^{-5} , we move on to Step (4), ending the iterative process.

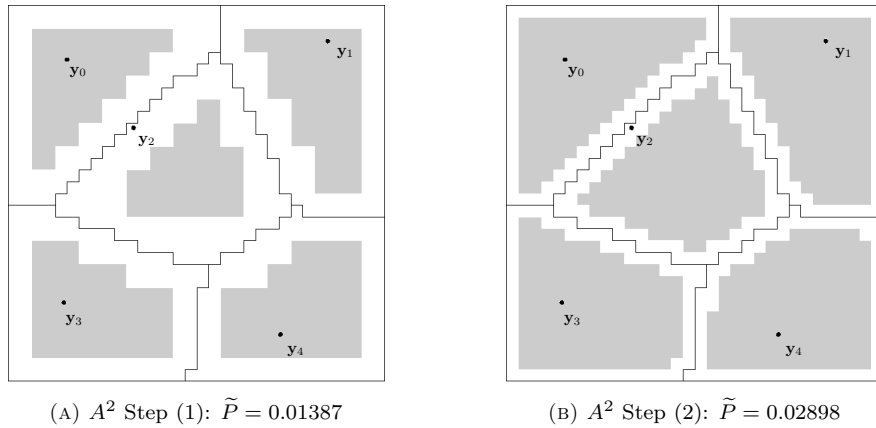


FIGURE 2. Iteration A^2 of Example 2.2 illustrated: $w_2 = 2^{-5}$

Next, we discuss the key elements of the algorithm: Steps (1), (4), and (5).

2.2.1. Step (1): solving the discrete optimal transport problem. Step (1) of the algorithm clearly emphasizes the characteristics required of an ideal transport solver for the boundary method: it needs only to approximate the correct solution, since misdirected points will be included in B^r , and their associated regions will be assigned after the next grid refinement. However, the approximation algorithm must be *fast* and possess reasonable scaling properties. To satisfy these requirements, and to bypass the shortcomings of standard

discrete approaches, we have turned to the distributed relaxation methods known as auction algorithms; see [3] and [4].

We chose to apply a new auction algorithm, the *general auction*, which we developed and presented in [27]. The general auction is so named because it is based directly on the (more general) real-valued transport problem, rather than the integer-valued assignment problem which forms the foundation of other auction algorithms. As described in [27], it offers significant performance advantages over other auction algorithms. Public domain C++ software implementing the general auction can be found on the Internet at [26].

2.2.2. Step (4): computing individual shift differences. Once we have reached a desired level of refinement for the boundary, we use the set B^r to identify $(n - 1)$ shift differences a_{ij} .

Suppose we have chosen to compute a specific shift difference a_{ij} . (The choice of i and j is discussed in Section 2.2.3 below.) In Step (1), we determined a map T showing us which $\mathbf{x} \in B^r$ were transported to \mathbf{y}_i . During Step (2), we used T to consider which of the neighbors of those points \mathbf{x} were transported to \mathbf{y}_j . Thus, we can create the set of unordered pairs

$$A_{ij}^r := \{ \{\mathbf{x}_i, \mathbf{x}_j\} \in B^r \mid T(\mathbf{x}_i) = \mathbf{y}_i, T(\mathbf{x}_j) = \mathbf{y}_j, \text{ and } \mathbf{x}_j \in N(\mathbf{x}_i) \}. \quad (2.10)$$

If $A_{ij}^r \neq \emptyset$, then by Theorem 3.26 (below), we must have $A_{ij}^r \neq \emptyset$.

As pointed out in Equation (2.6), all $\mathbf{x}_{ij} \in A_{ij}^r$ give us the identical exact value of a_{ij} . Hence, we can use any pair $\{\mathbf{x}_i, \mathbf{x}_j\} \in A_{ij}^r$ to compute an *approximate shift difference*

$$\tilde{a}_{ij} := g_{ij} \left(\frac{\mathbf{x}_i + \mathbf{x}_j}{2} \right) \quad (2.11)$$

In general, A_{ij}^r contains many pairs, and so our approximation of a_{ij} is significantly overdetermined. By considering one or more carefully-selected points from A_{ij}^r , we can minimize the error associated with the approximation \tilde{a}_{ij} .

2.2.3. Step (4): computing the shifts. As a consequence of (2.5), we know that each a_{ij} satisfies $a_{ij} = a_i - a_j$, and therefore

$$a_i = a_j + a_{ij}. \quad (2.12)$$

For all $i \in \mathbb{N}_n$, let $\tilde{a}_i = a_i + \alpha_i$, where α_i is the shift error. The first shift is assigned a value, and is therefore exact: $\tilde{a}_k = a_k$. Now suppose we use Equation (2.12) to approximate the value of some unknown shift a_i . If a_j is approximated with $\tilde{a}_j = a_j + \alpha_j$, and a_{ij} is approximated with $\tilde{a}_{ij} = a_{ij} + \alpha_{ij}$, then

$$\tilde{a}_i = \tilde{a}_j + \tilde{a}_{ij} = (a_j + \alpha_j) + (a_{ij} + \alpha_{ij}) = a_j + a_{ij} + (\alpha_j + \alpha_{ij}). \quad (2.13)$$

Thus, the error in our approximation of a_i could be as large as $|\alpha_j| + |\alpha_{ij}|$.

Inductively, the longer the path in our spanning tree H from v_k (the vertex corresponding to our initial shift) to v_i (the vertex corresponding to our target shift), the more error terms must be taken into account when approximating a_i . For this reason, we recommend computing the shifts using a greedy approach that always chooses the one with the largest number of adjacent regions whose shifts are still unknown.

Remark 2.3. The exact shifts $\{a_i\}_{i=1}^n$ correspond to a transport map giving the exact optimal solution of our semi-discrete problem. The approximated shifts $\{\tilde{a}_i\}_{i=1}^n$, unless generating the same shift differences, correspond to a transport map giving the exact optimal solution to a *different* semi-discrete problem, one whose measure ν at each \mathbf{y}_i , $i \in \mathbb{N}_n$, corresponds to the value of $\mu(\tilde{A}_i)$.

2.2.4. Step (5): approximating the Wasserstein distance. By the time we reach Step (5), the partial Wasserstein distance \tilde{P} includes the exact cost of all the identified interior regions. What remains is to approximate the cost of the regions associated with B^r .

Using the transport map T obtained during Step (1) of the r -th iteration, the approximated Wasserstein distance over \mathbf{x}^r is given by

$$P_{\mathbf{x}} := \int_{\mathbf{x}^r} c(\mathbf{z}, T(\mathbf{x})) d\mu(\mathbf{z}). \quad (2.14)$$

For each $\mathbf{x} \in B^r$ we can determine the set

$$\mathbf{y}_{\mathbf{x}} := \{\mathbf{y} \in Y \mid T(\mathbf{x}_n) = \mathbf{y} \text{ for some } \mathbf{x}_n \in \{\mathbf{x}\} \cup N(\mathbf{x})\}. \quad (2.15)$$

The maximum and minimum possible Wasserstein distance over \mathbf{x}^r equal

$$M_{\mathbf{x}} := \max_{\mathbf{y} \in \mathbf{y}_{\mathbf{x}}} \int_{\mathbf{x}^r} c(\mathbf{z}, \mathbf{y}) d\mu(\mathbf{z}) \quad \text{and} \quad m_{\mathbf{x}} := \min_{\mathbf{y} \in \mathbf{y}_{\mathbf{x}}} \int_{\mathbf{x}^r} c(\mathbf{z}, \mathbf{y}) d\mu(\mathbf{z}) \quad (2.16)$$

respectively. Hence, the error bound for the approximated Wasserstein distance over \mathbf{x}^r equals

$$\gamma_{\mathbf{x}} := \max\{M_{\mathbf{x}} - P_{\mathbf{x}}, P_{\mathbf{x}} - m_{\mathbf{x}}\}. \quad (2.17)$$

Summing over all B^r , the approximate Wasserstein distance equals

$$\tilde{P}^* := \tilde{P} + \sum_{\mathbf{x} \in B^r} P_{\mathbf{x}}, \quad (2.18)$$

and the error bound for the approximate Wasserstein distance is

$$\gamma^* := \sum_{\mathbf{x} \in B^r} \gamma_{\mathbf{x}}. \quad (2.19)$$

3. MATHEMATICAL SUPPORT

In this section, we provide mathematical support for the boundary method, assuming that all computations are solved exactly: both the discrete optimal transport problems handled by the general auction and the determinations of mass and Wasserstein distance for individual boxes (see Remark 2.1). We present three types of results: on the shift characterization, on our system of equations, and, finally, on the boundary method itself.

3.1. Semi-discrete optimal transport and the shift characterization. Here we examine the features of the shift characterization, defined in Section 1.4, and consider what they can tell us about the semi-discrete optimal transport problem itself.

First, in Lemmas 3.1 and 3.2, we develop theoretical support for the boundary method.

Lemma 3.1. *Fix $i \in \mathbb{N}_n$. If $\mathbf{x} \in A_i$ and $j \in \mathbb{N}_n$, $j \neq i$, then the following hold:*

$$(3.1) \quad g_{ij}(\mathbf{x}) \leq a_i - a_j,$$

$$(3.2) \quad g_{ij}(\mathbf{x}) = a_i - a_j \quad \iff \quad \mathbf{x} \in A_{ij}, \text{ and}$$

$$(3.3) \quad g_{ij}(\mathbf{x}) < a_i - a_j \quad \iff \quad \mathbf{x} \in A_i \setminus A_j.$$

Proof. Let us show Equation (3.1). By the definitions of A_i and F ,

$$a_i - c(\mathbf{x}, \mathbf{y}_i) = F(\mathbf{x}) \geq a_j - c(\mathbf{x}, \mathbf{y}_j).$$

Rearranging terms gives

$$c(\mathbf{x}, \mathbf{y}_i) - c(\mathbf{x}, \mathbf{y}_j) \leq a_i - a_j.$$

To show Equation (3.2), first note that Section 2.1 already explains how $\mathbf{x} \in A_{ij}$ implies $g_{ij}(\mathbf{x}) = a_i - a_j$. Consider the converse: Assume that $g_{ij}(\mathbf{x}) = a_i - a_j$. Rewriting, we find that $a_j - c(\mathbf{x}, \mathbf{y}_j) = a_i - c(\mathbf{x}, \mathbf{y}_i) = F(\mathbf{x})$. This implies $\mathbf{x} \in A_j$, and since $\mathbf{x} \in A_i$, therefore $\mathbf{x} \in A_{ij}$. Equation (3.3) is a consequence of Equations (3.1) and (3.2). \square

Lemma 3.2. *Suppose c satisfies the triangle inequality. For all $i, j \in \mathbb{N}_n$, $i \neq j$,*

(a) *If $c(\mathbf{y}_i, \mathbf{y}_j) = a_i - a_j$, then $A_j \subseteq A_{ij}$.*

(b) *If $c(\mathbf{y}_i, \mathbf{y}_j) < a_i - a_j$, then $A_j = \emptyset$.*

Proof. For Part (a), because c satisfies the triangle inequality, for all $\mathbf{x} \in A$,

$$(3.4) \quad \begin{aligned} c(\mathbf{x}, \mathbf{y}_i) &\leq c(\mathbf{x}, \mathbf{y}_j) + c(\mathbf{y}_i, \mathbf{y}_j) \\ c(\mathbf{x}, \mathbf{y}_i) &\leq c(\mathbf{x}, \mathbf{y}_j) + a_i - a_j \\ a_j - c(\mathbf{x}, \mathbf{y}_j) &\leq a_i - c(\mathbf{x}, \mathbf{y}_i). \end{aligned}$$

Suppose $\mathbf{x} \in A_j$. Then $a_i - c(\mathbf{x}, \mathbf{y}_i) \geq a_j - c(\mathbf{x}, \mathbf{y}_j) = F(\mathbf{x})$. Because F is defined as the maximum such difference, this implies $a_i - c(\mathbf{x}, \mathbf{y}_i) = F(\mathbf{x})$, and so $\mathbf{x} \in A_i$. Further, since \mathbf{x} is an element of A_i and A_j , $\mathbf{x} \in A_{ij}$. Therefore, $A_j \subseteq A_{ij}$.

To show (b), note that (3.4) now gives $a_j - c(\mathbf{x}, \mathbf{y}_j) < a_i - c(\mathbf{x}, \mathbf{y}_i)$. Hence, for all $\mathbf{x} \in A$, $F(\mathbf{x}) \geq a_i - c(\mathbf{x}, \mathbf{y}_i) > a_j - c(\mathbf{x}, \mathbf{y}_j)$. Therefore, $A_j = \emptyset$. \square

Lemma 3.3. $F(\mathbf{x})$ is a continuous function of \mathbf{x} .

Proof. The ground cost c is defined as a continuous function in $X \times Y$. Thus, for all $i \in \mathbb{N}_n$, $a_i - c(x, y_i)$ is a continuous function of \mathbf{x} . Since F is the maximum of a finite set of continuous functions, F is itself a continuous function of \mathbf{x} . \square

Theorem 3.4 (F μ -partitions A). *Suppose we have a semi-discrete transport problem, as described in Section 1.3. Let F be as defined in Equation (1.18), and the sets A_i as defined in Equation (1.19) for $i \in \mathbb{N}_n$. Then F μ -partitions the set A (or F is a μ -partition); that is,*

- (1) for all $i \in \mathbb{N}_n$, $\mu(A_i) > 0$,
- (2) $\sum_{i=1}^n \mu(A_i) = \mu(A)$, and
- (3) for all $i, j \in \mathbb{N}_n$, $i \neq j$, $\mu(A_{ij}) = 0$.

Proof. Assume F and the sets A_i are defined as given. Because μ is a probability density function, $\mu(A) = 1$. For all $i \in \mathbb{N}_n$, $\mu(A_i) = \nu(\mathbf{y}_i) > 0$, and hence

$$\sum_{i=1}^n \mu(A_i) = \sum_{i=1}^n \nu(\mathbf{y}_i) = 1 = \mu(A).$$

Finally, for any μ -measurable set $S \subseteq X$, $S = S_1 \cup S_2$ implies $\mu(S_1) + \mu(S_2) = \mu(S) + \mu(S_1 \cap S_2)$, and since $\mu(X) < \infty$, $\mu(S) = \mu(S_1) + \mu(S_2) - \mu(S_1 \cap S_2)$. Proceeding inductively, it follows that

$$S = \bigcup_{i=1}^n S_i, \text{ all } \mu\text{-measurable} \quad \implies \quad \mu(S) = \sum_{i=1}^n \mu(S_i) - \sum_{i=1}^n \sum_{\substack{j=1 \\ j \neq i}}^n \mu(S_i \cap S_j).$$

Thus,

$$\begin{aligned} 1 = \mu(A) &= \sum_{i=1}^n \mu(A_i) - \sum_{i=1}^n \sum_{\substack{j=1 \\ j \neq i}}^n \mu(A_{ij}) \\ &= \sum_{i=1}^n \nu(\mathbf{y}_i) - \sum_{i=1}^n \sum_{\substack{j=1 \\ j \neq i}}^n \mu(A_{ij}) = 1 - \sum_{i=1}^n \sum_{\substack{j=1 \\ j \neq i}}^n \mu(A_{ij}). \end{aligned}$$

Therefore,

$$\sum_{i=1}^n \sum_{\substack{j=1 \\ j \neq i}}^n \mu(A_{ij}) = 0,$$

and since μ is nonnegative, then for all $i, j \in \mathbb{N}_n$, $i \neq j$, $\mu(A_{ij}) = 0$. \square

Definition 3.5. We say a transport plan π is *consistent with the shift characterization* if π has an associated transport map T , a function F , as described in Equation (1.18), and sets $\{A_i\}_{i=1}^n$, as described in Equation (1.19), such that for all $\mathbf{x} \in A$,

$$\mathbf{x} \in \mathring{A}_i \text{ for some } i \in \mathbb{N}_n \quad \implies \quad T(\mathbf{x}) = \mathbf{y}_i. \quad (3.5)$$

In other words, T agrees with the μ -partition F on $A \setminus B$.

Theorem 3.6 (The optimal transport map is unique μ -a.e.). *Given a semi-discrete transport problem, let π^* and $\tilde{\pi}^*$ be optimal transport plans that are both consistent with the shift characterization. If T is a transport map associated with π^* , and \tilde{T} a transport map associated with $\tilde{\pi}^*$, then $T = \tilde{T}$ except on a set of μ -measure zero.*

Proof. Assume to the contrary that T and \tilde{T} differ on a set of μ -positive measure. We will show that the difference between the Wasserstein distances $P(\tilde{\pi}^*)$ and $P(\pi^*)$ must be non-zero, thereby establishing the desired contradiction: at least one of π^* and $\tilde{\pi}^*$ is not optimal.

Because T is consistent with the shift characterization, there exist F and $\{A_i\}_{i=1}^n$ that satisfy the definitions in Equations (1.18) and (1.19). Similarly, we have \tilde{F} and $\{\tilde{A}_i\}_{i=1}^n$ for \tilde{T} . Let $\{a_i\}_{i=1}^n$ be the set of shifts associated with F , and $\{\tilde{a}_i\}_{i=1}^n$ the shifts associated with \tilde{F} . For all $i, j \in \mathbb{N}_n, i \neq j$, define

$$X_{ij} := \left\{ \mathbf{x} \in A \mid T(\mathbf{x}) = \mathbf{y}_i \quad \text{and} \quad \tilde{T}(\mathbf{x}) = \mathbf{y}_j \right\}.$$

Since F μ -partitions A , $\mu(A_{ij}) = 0$. The Wasserstein distance is only affected by sets of positive measure, so without loss of generality assume $X_{ij} \cap A_{ij} = \emptyset$.

With respect to the transformation from π^* to the map $\tilde{\pi}^*$, the change in Wasserstein distance over the set X_{ij} equals

$$\begin{aligned} \Delta P_{ij} &:= \int_{X_{ij}} c(\mathbf{x}, \tilde{T}(\mathbf{x})) d\mu(\mathbf{x}) - \int_{X_{ij}} c(\mathbf{x}, T(\mathbf{x})) d\mu(\mathbf{x}) \\ &= \int_{X_{ij}} [c(\mathbf{x}, \mathbf{y}_j) - c(\mathbf{x}, \mathbf{y}_i)] d\mu(\mathbf{x}). \end{aligned}$$

Since $X_{ij} \cap A_{ij} = \emptyset$, $\mathbf{x} \in X_{ij}$ implies $\mathbf{x} \in A_i \setminus A_j$. Hence, by Equation (3.3),

$$\forall \mathbf{x} \in X_{ij}, \quad g_{ij}(\mathbf{x}) < a_i - a_j.$$

Therefore, for all $i, j \in \mathbb{N}_n, i \neq j$ implies $\Delta P_{ij} \geq (a_j - a_i)\mu(X_{ij})$, with equality if and only if $\mu(X_{ij}) = 0$.

Let

$$X_i = \bigcup_{\substack{j=1 \\ j \neq i}}^n X_{ij} \quad \text{and} \quad \Delta P_i = \sum_{\substack{j=1 \\ j \neq i}}^n \Delta P_{ij}.$$

If i, j , and k are pairwise distinct, by definition $X_{ij} \cap X_{ik} = \emptyset$. Therefore

$$\mu(X_i) = \sum_{\substack{j=1 \\ j \neq i}}^n \mu(X_{ij}) \quad \text{and} \quad \Delta P_i \geq \sum_{\substack{j=1 \\ j \neq i}}^n (a_j - a_i)\mu(X_{ij}).$$

By the definition of the shift characterization, we must have $\mu(A_i) = \mu(\tilde{A}_i)$. Thus,

$$\mu(A_i) = \mu(\tilde{A}_i) = \mu \left((A_i \setminus X_i) \cup \left(\bigcup_{\substack{j=1 \\ j \neq i}}^n X_{ji} \right) \right),$$

and because the sets are disjoint, this implies

$$\mu(A_i) = \mu(A_i) - \mu(X_i) + \sum_{\substack{j=1 \\ j \neq i}}^n \mu(X_{ji}), \quad \text{and therefore} \quad \mu(X_i) = \sum_{\substack{j=1 \\ j \neq i}}^n \mu(X_{ji}).$$

Since T and \tilde{T} differ on a set of positive measure, we know there exists at least one pair $i, j \in \mathbb{N}_n$ such that $i \neq j$ and $\mu(X_{ij}) > 0$. For that i and j , $\Delta P_{ij} > (a_j - a_i)\mu(X_{ij})$, which implies

$$\Delta P_i > \sum_{\substack{j=1 \\ j \neq i}}^n (a_j - a_i)\mu(X_{ij}).$$

Thus,

$$\Delta P := \sum_{i=1}^n \Delta P_i > \sum_{i=1}^n \left(\sum_{\substack{j=1 \\ j \neq i}}^n (a_j - a_i)\mu(X_{ij}) \right).$$

By rearranging terms and indexing appropriately

$$\sum_{i=1}^n \left(\sum_{\substack{j=1 \\ j \neq i}}^n (a_j - a_i)\mu(X_{ij}) \right) = \left(\sum_{i=1}^n \sum_{\substack{j=1 \\ j \neq i}}^n a_j \mu(X_{ij}) \right) - \sum_{i=1}^n a_i \left(\sum_{\substack{j=1 \\ j \neq i}}^n \mu(X_{ij}) \right)$$

$$\begin{aligned}
&= \left(\sum_{j=1}^n \sum_{\substack{i=1 \\ j \neq i}}^n a_i \mu(X_{ji}) \right) - \sum_{i=1}^n a_i \mu(X_i) = \left(\sum_{i=1}^n \sum_{\substack{j=1 \\ j \neq i}}^n a_i \mu(X_{ji}) \right) - \sum_{i=1}^n a_i \mu(X_i) \\
&= \sum_{i=1}^n a_i \left(\sum_{\substack{j=1 \\ j \neq i}}^n \mu(X_{ji}) \right) - \sum_{i=1}^n a_i \mu(X_i) = \sum_{i=1}^n a_i \left(-\mu(X_i) + \sum_{\substack{j=1 \\ j \neq i}}^n \mu(X_{ji}) \right) \\
&= \sum_{i=1}^n a_i(0) = 0.
\end{aligned}$$

Thus, $\Delta P > 0$, which implies $P(\tilde{\pi}^*) > P(\pi^*)$. This contradicts the definition of $\tilde{\pi}^*$ as optimal. Therefore \tilde{T} and T must differ only on sets of μ -measure zero. \square

3.2. Existence of functionally independent boundary equations. To prove the existence of $(n-1)$ functionally independent equations of the form shown in Equation (2.6), we will investigate the structure of the boundary set using a connected graph G defined as follows:

Definition 3.7. Let G be a graph with n vertices v_1, \dots, v_n . The edge (v_i, v_j) is contained in the edge set of G if and only if A_{ij} is non-empty. We refer to G as the *adjacency graph* of our transport problem.

Theorem 3.8. G is a connected graph.

Proof. Assume to the contrary that G is not a connected graph. Then we can write G as the union of two disjoint subgraphs, $G = G_1 \cup G_2$, such that no vertex v_1 in G_1 has a path connecting it to any vertex v_2 in G_2 .

Define

$$A_1 := \bigcup_{v_i \in G_1} A_i \quad \text{and} \quad A_2 := \bigcup_{v_j \in G_2} A_j.$$

Because G_1 and G_2 are disjoint, and no paths connect them, it follows that $A_1 \cap A_2 = \emptyset$. Since the union of G_1 and G_2 is G , $A_1 \cup A_2 = A$.

Suppose $A_i \subseteq A_1$, $A_j \subseteq A_2$. Then $A_{ij} = \emptyset$. A is a closed and bounded set, and the definition given in Equation (1.19) implies that A_i and A_j must also be closed and bounded. Thus, A_i and A_j are disjoint compact sets in the Hausdorff space \mathbb{R}^d . This implies A_i and A_j are separated by some positive distance ϵ_{ij} . Because this is true for all $A_i \subseteq A_1$ and $A_j \subseteq A_2$, there exists $\epsilon > 0$, the minimum over all such ϵ_{ij} .

Let $\mathbf{x}_1 \in A_1$, $\mathbf{x}_2 \in A_2$, and for all $t \in [0, 1]$, define

$$\mathbf{x}_t = (1-t)\mathbf{x}_1 + t\mathbf{x}_2.$$

Because $\epsilon > 0$, there exists $(t_0, t_1) \subseteq [0, 1]$, $|t_1 - t_0| \geq \epsilon$, such that $t \in (t_0, t_1)$ implies $\mathbf{x}_t \notin A_1 \cup A_2 = A$. This contradicts the convexity of A . Hence, G is connected. \square

Corollary 3.9. If $i \in \mathbb{N}_n$, there exists $j \in \mathbb{N}_n$, such that $j \neq i$ and $A_{ij} \neq \emptyset$.

Proof. Assume the contrary for some i . Since $n \geq 2$, G includes at least two vertices, and v_i is disconnected from the rest of G , which contradicts Theorem 3.8. \square

Corollary 3.10. The boundary set B is nonempty, and for each $\mathbf{x} \in B$, there exist $i, j \in \mathbb{N}_n$ such that $i \neq j$ and $\mathbf{x} \in A_{ij}$.

Proof. This follows from Corollary 3.9 and the definition of B in Equation (2.2). \square

Theorem 3.11. Let G be the adjacency graph of the transport problem, and let H be a subgraph of G that includes all n vertices. Define the system of equations

$$S := \{a_i - a_j = a_{ij} \mid (v_i, v_j) \in \text{the edge set of } H\}. \quad (3.6)$$

The system of equations S is functionally independent with respect to the shifts $\{a_i\}_{i=1}^n$ if and only if H contains no cycles.

Proof. (\implies) Suppose H contains the cycle $(v_{i_1}, v_{i_2}, \dots, v_{i_k}, v_{i_1})$. Then S contains the linear system

$$M \begin{bmatrix} a_{i_1} \\ \vdots \\ a_{i_{k-1}} \\ a_{i_k} \end{bmatrix} = \begin{bmatrix} a_{i_1 i_2} \\ \vdots \\ a_{i_{k-1} i_k} \\ a_{i_k i_1} \end{bmatrix}, \quad \text{where } M = \begin{bmatrix} 1 & -1 & & & \\ & & \ddots & & \\ & & & \ddots & \\ & & & & 1 & -1 \\ -1 & & & & & 1 \end{bmatrix}.$$

Because $\det(M) = 0$, we know S is functionally dependent.

(\impliedby) Suppose instead that S is functionally dependent. Given the form of the equations in S , we can assume without loss of generality that S contains the equations $a_{i_j i_{j+1}} = a_{i_j} - a_{i_{j+1}}$, $\forall j \in \mathbb{N}_{k-1}$, and that $a_{i_1 i_k} = a_{i_1} - a_{i_k}$ is also in S . By the definition of S , these equations imply that the edges $(v_1, v_2), (v_2, v_3), \dots, (v_{k-1}, v_k)$, and (v_k, v_1) are contained in H . Together, these edges generate the cycle $(v_{i_1}, v_{i_2}, \dots, v_{i_k}, v_{i_1})$, so H contains at least one cycle. \square

Theorem 3.12. *There exists at least one system of exactly $(n-1)$ equations of the form $a_i - a_j = a_{ij}$ that is functionally independent with respect to the set of shifts $\{a_i\}_{i=1}^n$. No system of n independent equations exists.*

Proof. Because G is a connected graph, we can always create a spanning tree H that is a subgraph of G . Let S be the corresponding set of linear equations, defined as described in (3.6). As a spanning tree, H contains $(n-1)$ edges and H has no cycles, so by Theorem 3.11, we know S contains exactly $(n-1)$ functionally independent equations.

Suppose a set S of n functionally independent equations exists, all of the form $a_i - a_j = a_{ij}$. Because there are n unknowns in the set of shifts, there is exactly one solution set $\{a_i\}_{i=1}^n$. Fix $\sigma \neq 0$ and for all $i \in \mathbb{N}_n$, define $\tilde{a}_i = a_i + \sigma$. For each equation in S , $\tilde{a}_i - \tilde{a}_j = a_i - a_j = a_{ij}$. Thus, $\{\tilde{a}_i\}_{i=1}^n$ is also a solution to S . This contradicts the uniqueness of $\{a_i\}_{i=1}^n$, and therefore no such set of n functionally independent equations exists. \square

3.3. Discretization for the boundary method. In the first two subsections below, we give some results on how the grid-points interact with the underlying space. In sections 3.3.3 and 3.3.4 we present error bounds. In section 3.3.5 we consider issues of volume and containment: here we ensure that one can have $B \subseteq \bar{B}^r$ for all r , and show that $|\bar{B}^r| \rightarrow 0$ as $r \rightarrow \infty$. Finally, Section 3.3.6 puts bounds on the error for the Wasserstein distance approximation.

3.3.1. Discretization definitions. As described in Section 2.2, we discretize the region A using a regular Cartesian grid, and refine the grid over multiple iterations, with the aim of refining only the grid region containing the boundary set.

Let $r \in \mathbb{N}$ be the current discretization level, and $w = w_r$ be the *width* of the discretization at level r . Let A^r be the r -th *point set*, the set of points \mathbf{x} included in the r -th discretization of A . Since we discard boxes of μ -measure zero during the transport step, assume without loss of generality that $\mu(\mathbf{x}^r) > 0$ for all $\mathbf{x} \in A^r$. Let $A_i^r = A_i \cap A^r$ for $i \in \mathbb{N}_n$.

Let \mathcal{V} be the set of adjacency vectors for all discretizations of A . The adjacency vectors must satisfy the following essential properties:

- (1) If $\mathbf{v} = (v_1, \dots, v_d) \in \mathcal{V}$, then $|v_i| \leq 1$ for all $i \in \{1, \dots, d\}$.
- (2) $\mathbf{0} \notin \mathcal{V}$.
- (3) $\mathbf{v} \in \mathcal{V}$ implies $-\mathbf{v} \in \mathcal{V}$.

We choose \mathcal{V} to be the set of linear combinations of the standard unit vectors, e_1, \dots, e_d , with coefficients restricted to ± 1 . To satisfy Property (2), we specifically exclude the zero vector from the set, and so $|\mathcal{V}| = 3^d - 1$. If $d = 2$, \mathcal{V} equals

$$\mathcal{V} := \{(-1, -1), (0, -1), (-1, 0), (-1, 1), (1, -1), (1, 0), (0, 1), (1, 1)\}. \quad (3.7)$$

The properties of the adjacency vectors are required in order to assure that, for all r and all $\mathbf{x} \in A^r$, the points in A^r that are adjacent to \mathbf{x} constitute a subset of the *neighbors* of \mathbf{x} ,

$$N(\mathbf{x}) := \{\mathbf{x} + w_r \mathbf{v} \mid \mathbf{v} \in \mathcal{V}\}. \quad (3.8)$$

Lemma 3.13. *If $\mathbf{x} \in N(\mathbf{x}_0)$, then $\mathbf{x}_0 \in N(\mathbf{x})$.*

Proof. This follows from Equation (3.8) and Property (3) of the adjacency vectors. \square

We now formalize our idea of the r -th interior and boundary point sets used in our discretization. For all $i \in \mathbb{N}_n$, define the r -th iteration *interior point set* associated with A_i as

$$\hat{A}_i^r := \{\mathbf{x} \in A_i^r \mid \forall \mathbf{v} \in \mathcal{V}, \mathbf{x} + w_r \mathbf{v} \in A_j^r \implies j = i\}. \quad (3.9)$$

Define the r -th *boundary point set* as

$$B^r := A^r \setminus \bigcup_{i=1}^n \hat{A}_i^r, \quad (3.10)$$

and let $B_i^r := B^r \cap A_i$ for all $i \in \mathbb{N}_n$. The r -th *evaluation region*, the subset of A enclosed by the discretization A^r , is defined as

$$\bar{A}^r := \{\mathbf{x}^r \mid \mathbf{x} \in A^r\}, \quad (3.11)$$

and the r -th *boundary region*, the subset of A enclosed by the boundary point set B^r , is given by

$$\bar{B}^r := \{\mathbf{x}^r \mid \mathbf{x} \in B^r\}. \quad (3.12)$$

3.3.2. Distance bounds. Though the discretization is fully defined, it still needs to be related back to the sets A_{ij} and the boundary set B . To do this, we first bound the distance separating B^r and A_{ij} .

Theorem 3.14. *Suppose $B_i^r \neq \emptyset$. For each $\mathbf{x}_i \in B_i^r$, either $\mathbf{x}_i \in \text{edg}(A^r)$ or there exists a point $\mathbf{x}_j = \mathbf{x}_i + w_r \mathbf{v}$, with $\mathbf{v} \in \mathcal{V}$, such that $\mathbf{x}_j \in B_j^r$ for some $j \neq i$. Thus, if $\mathbf{x}_i \notin \text{edg}(A^r)$, the distance from \mathbf{x}_i to the set A_{ij} , as measured with respect to the ground cost c , is bounded above by $c(\mathbf{x}_i, \mathbf{x}_j)$.*

Proof. Assume $\mathbf{x}_i \in B_i^r \setminus \text{edg}(A^r)$. By the definition of B^r , there exists $\mathbf{x}_j = \mathbf{x}_i + w_r \mathbf{v} \in A_j^r \cup N(\mathbf{x}_0)$ for some $j \neq i$. By Lemma 3.13, $\mathbf{x}_i \in N(\mathbf{x}_j)$, and since $\mathbf{x}_i \in A_i^r$, we have $\mathbf{x}_j \in B_j^r$. Thus, $\mathbf{x}_i \in A$ and $\mathbf{x}_j \in A$, and because A is convex, this implies

$$\{t\mathbf{x}_i + (1-t)\mathbf{x}_j \mid t \in [0, 1]\} \subseteq A.$$

By Lemma 3.3, F is continuous on A . Therefore, because $\mathbf{x}_i \in A_i$ and $\mathbf{x}_j \in A_j$, there exists $t_* \in [0, 1]$ such that $\mathbf{b} = t_* \mathbf{x}_i + (1-t_*)\mathbf{x}_j \in A_{ij}$. Note that $\mathbf{b} = \mathbf{x}_i + (1-t_*)w_r \mathbf{v}$, so all three points are collinear. Applying the ℓ_2 norm, we have

$$\|\mathbf{b} - \mathbf{x}_i\|_2 = \|(1-t_*)w_r \mathbf{v}\|_2 = (1-t_*)\|w_r \mathbf{v}\|_2 \leq \|w_r \mathbf{v}\|_2 = \|\mathbf{x}_j - \mathbf{x}_i\|_2.$$

Since c is an admissible cost function and $\|\mathbf{b} - \mathbf{x}_i\|_2 \leq \|\mathbf{x}_j - \mathbf{x}_i\|_2$, this implies $c(\mathbf{x}_i, \mathbf{b}) \leq c(\mathbf{x}_i, \mathbf{x}_j)$. \square

Because we can bound the ground cost between the points in $B^r \setminus \text{edg}(A^r)$ and the set A_{ij} in terms of the ground cost between neighboring points, it is worth identifying a bound on that ground cost between neighbors.

First, we ensure that some bound exists for every ground cost function and iteration r .

Lemma 3.15. *For all $\mathbf{x}_i \in B_i^r$ and $\mathbf{x}_j \in B_j^r$, where $i, j \in \mathbb{N}_n$ and $i \neq j$, if $\mathbf{x}_j \in N(\mathbf{x}_i)$, then $c(\mathbf{x}_i, \mathbf{x}_j) < M_r$ for some bounded value M_r .*

Proof. Let \mathbf{x}_i and \mathbf{x}_j be defined as above. By applying the definition given in Equation (3.10), $\mathbf{x}_j = \mathbf{x}_i + w_r \mathbf{v}$ for some $\mathbf{v} \in \mathcal{V}$. Further, we can assume without loss of generality that $c(\mathbf{x}_i, \mathbf{x}_j)$ is maximized among the finite set of neighbors of \mathbf{x}_i . Let M_r be defined as the maximum of all such ground costs over the set of points in B^r :

$$M_r = \max_{\substack{\mathbf{x}_i \in B_i^r \\ 1 \leq i \leq n}} \max_{\{\mathbf{x}_j = \mathbf{x}_i + w_r \mathbf{v} \in B_j^r \mid j \neq i\}} c(\mathbf{x}_i, \mathbf{x}_j). \quad (3.13)$$

Because M_r is the maximum of a finite set of finite values, $M_r < \infty$. \square

We can give a specific ground cost bound in terms of w_r for neighbors \mathbf{x}_0 and \mathbf{x}_1 when \mathcal{V} is our Cartesian grid and c is a polynomial combination of ℓ_p functions with positive coefficients.

Corollary 3.16. *Suppose \mathcal{V} defines the Cartesian grid on \mathbb{R}^d , as described above, and c is a polynomial combination of ℓ_p functions with positive coefficients:*

$$c = \sum_{s=1}^{\sigma} k_s \ell_{p_s}^{q_s} \text{ such that } k_s, p_s, q_s > 0 \text{ for all } s \in \mathbb{N}_\sigma. \quad (3.14)$$

Let $q = \min_{1 \leq s \leq \sigma} q_s$. Then the maximum M_r , as described in Lemma 3.15, satisfies

$$M_r \leq (w_r)^q \sum_{s=1}^{\sigma} k_s (w_r)^{q_s - q} (d)^{q_s / p_s}. \quad (3.15)$$

Proof. Let $\mathbf{x} \in B^r$ and fix $s \in \mathbb{N}_\sigma$. For all $\mathbf{v} \in V$, the subcost $c_s = \ell_{p_s}^{q_s}$ can be computed as

$$c_s(\mathbf{x}, \mathbf{x} + w_r \mathbf{v}) = \|(\mathbf{x} + w_r \mathbf{v}) - \mathbf{x}\|_{p_s}^{q_s} = w_r^{q_s} \|\mathbf{v}\|_{p_s}^{q_s}.$$

For our Cartesian grid \mathcal{V} , $\|\mathbf{v}\|_{p_s}^{q_s}$ achieves its maximum when $\mathbf{v} = \mathbb{1}_d$, so

$$w_r^{q_s} \|\mathbf{v}\|_{p_s}^{q_s} \leq w_r^{q_s} \|\mathbb{1}_d\|_{p_s}^{q_s} = \left(w_r d^{1/p_s}\right)^{q_s}.$$

Thus,

$$c(\mathbf{x}, \mathbf{x} + w_r \mathbf{v}) = \sum_{s=1}^{\sigma} k_s c_s(\mathbf{x}, \mathbf{x} + w_r \mathbf{v}) \leq \sum_{s=1}^{\sigma} k_s \left(w_r d^{1/p_s}\right)^{q_s}.$$

By determining $q = \min_{1 \leq s \leq \sigma} q_s > 0$, and factoring out w_r^q , we arrive at (3.15). \square

3.3.3. Error bounds for shift differences. In order to bound the error on the Wasserstein distance, we merely require a finite bound on the errors for the individual shift differences, a_{ij} . However, accurately computing the shift differences themselves is also important, and for that reason, we also present theorems that more finely bound the error on a_{ij} for important ground cost functions. Because estimates are generated using one or more computations of $g_{ij}(\mathbf{x})$, the magnitude of these errors is dependent on the point(s) chosen.

Theorem 3.17. *Let $\mathbf{x} \in A$ and $i, j \in \mathbb{N}_n$ such that $i \neq j$. The error resulting from approximating a_{ij} at \mathbf{x} is bounded above by $|\alpha_{ij}(\mathbf{x})|$, where*

$$\alpha_{ij}(\mathbf{x}) := [c(\mathbf{x}, \mathbf{y}_i) - c(\mathbf{b}, \mathbf{y}_i)] + [c(\mathbf{b}, \mathbf{y}_j) - c(\mathbf{x}, \mathbf{y}_j)], \quad (3.16)$$

and \mathbf{b} is the point in A_{ij} nearest to \mathbf{x} with respect to the ground cost.

Proof. Assume $\mathbf{b} \in A_{ij}$ is the closest point in A_{ij} to \mathbf{x} . Then

$$c(\mathbf{b}, \mathbf{y}_i) - c(\mathbf{b}, \mathbf{y}_j) = g_{ij}(\mathbf{b}) = a_{ij}.$$

For every $\mathbf{x} \in A$, there exists some $\alpha_{ij}(\mathbf{x}) \in \mathbb{R}$ such that

$$c(\mathbf{x}, \mathbf{y}_i) - c(\mathbf{x}, \mathbf{y}_j) = a_{ij} + \alpha_{ij}.$$

By rearrangement and substitution, we have

$$\begin{aligned} \alpha_{ij}(\mathbf{x}) &= -a_{ij} + c(\mathbf{x}, \mathbf{y}_i) - c(\mathbf{x}, \mathbf{y}_j) \\ &= -[c(\mathbf{b}, \mathbf{y}_i) - c(\mathbf{b}, \mathbf{y}_j)] + c(\mathbf{x}, \mathbf{y}_i) - c(\mathbf{x}, \mathbf{y}_j) \\ &= [c(\mathbf{x}, \mathbf{y}_i) - c(\mathbf{b}, \mathbf{y}_i)] + [c(\mathbf{b}, \mathbf{y}_j) - c(\mathbf{x}, \mathbf{y}_j)]. \end{aligned} \quad \square$$

Theorem 3.18. *Suppose \mathcal{V} is our Cartesian grid and c is a polynomial combination of ℓ_p functions with positive coefficients, as defined in Equation (3.14). For any $\mathbf{x} \in A$ and $i, j \in \mathbb{N}_n$ such that $i \neq j$, $|\alpha_{ij}(\mathbf{x})| < \infty$.*

Proof. Because all costs are nonnegative, and achieve their maximum with $c(\mathbf{0}, l\mathbb{1}_d)$,

$$\begin{aligned} |\alpha_{ij}(\mathbf{x})| &= |[c(\mathbf{x}, \mathbf{y}_i) - c(\mathbf{b}, \mathbf{y}_i)] + [c(\mathbf{b}, \mathbf{y}_j) - c(\mathbf{x}, \mathbf{y}_j)]| \\ &\leq |c(\mathbf{0}, l\mathbb{1}_d) - 0| + |c(\mathbf{0}, l\mathbb{1}_d) - 0| \\ &= 2c(\mathbf{0}, l\mathbb{1}_d) = 2 \sum_{s=1}^{\sigma} k_s \left(ld^{1/p_s}\right)^{q_s} < \infty. \end{aligned} \quad \square$$

Theorem 3.19. *Assume that, in addition to satisfying the ground cost properties, c satisfies the triangle inequality. If a_{ij} is estimated using $\mathbf{x} \in A$, then $|\alpha_{ij}(\mathbf{x})| \leq 2c(\mathbf{x}, \mathbf{b})$, where \mathbf{b} is the point in A_{ij} nearest to \mathbf{x} with respect to the ground cost.*

Proof. Applying (3.16),

$$\begin{aligned} |\alpha_{ij}(\mathbf{x})| &= |[c(\mathbf{x}, \mathbf{y}_i) - c(\mathbf{b}, \mathbf{y}_i)] + [c(\mathbf{b}, \mathbf{y}_j) - c(\mathbf{x}, \mathbf{y}_j)]| \\ &\leq |c(\mathbf{x}, \mathbf{y}_i) - c(\mathbf{b}, \mathbf{y}_i)| + |c(\mathbf{b}, \mathbf{y}_j) - c(\mathbf{x}, \mathbf{y}_j)|. \end{aligned}$$

Since c satisfies the triangle inequality,

$$c(\mathbf{x}, \mathbf{y}_i) - c(\mathbf{b}, \mathbf{y}_i) \leq c(\mathbf{x}, \mathbf{b}) + c(\mathbf{b}, \mathbf{y}_i) - c(\mathbf{b}, \mathbf{y}_i) = c(\mathbf{x}, \mathbf{b}).$$

Thus,

$$|c(\mathbf{x}, \mathbf{y}_i) - c(\mathbf{b}, \mathbf{y}_i)| \leq |c(\mathbf{x}, \mathbf{b})| = c(\mathbf{x}, \mathbf{b}),$$

and, by a similar line of reasoning, $|c(\mathbf{b}, \mathbf{y}_j) - c(\mathbf{x}, \mathbf{y}_j)| \leq c(\mathbf{x}, \mathbf{b})$. Therefore,

$$|\alpha_{ij}(\mathbf{x})| \leq |c(\mathbf{x}, \mathbf{y}_i) - c(\mathbf{b}, \mathbf{y}_i)| + |c(\mathbf{b}, \mathbf{y}_j) - c(\mathbf{x}, \mathbf{y}_j)| \leq 2c(\mathbf{x}, \mathbf{b}). \quad \square$$

In addition to bounding the error for individual points \mathbf{x} , we can also establish meaningful global bounds.

Definition 3.20. Let α_{\max} be the maximum value of $|\alpha_{ij}(\mathbf{x})|$ over all $\mathbf{x} \in \bar{B}^r$ and $i, j \in \mathbb{N}_n$, such that: (1) $i \neq j$, (2) $\mathbf{x} \in \mathbf{x}_i^r$ for some $\mathbf{x}_i \in B_i^r$, and (3) $B_j^r \cap N(\mathbf{x}_i) \neq \emptyset$.

Lemma 3.21. Suppose \mathcal{V} is our Cartesian grid and c is a polynomial combination of ℓ_p functions with positive coefficients, as defined in Equation (3.14). Then $\alpha_{\max} < \infty$.

Proof. As shown in Theorem 3.18, for all appropriate \mathbf{x} , i , and j ,

$$|\alpha_{ij}(\mathbf{x})| \leq 2 \sum_{s=1}^{\sigma} k_s \left(ld^{1/p_s} \right)^{q_s}.$$

Since this bound is independent of \mathbf{x} , i , and j , it follows that

$$\alpha_{\max} \leq 2 \sum_{s=1}^{\sigma} k_s \left(ld^{1/p_s} \right)^{q_s} < \infty. \quad \square$$

Theorem 3.22. If c is a norm, then $\alpha_{\max} \leq 2\delta$, where δ is the maximum ground cost for a pair of neighboring points in the grid discretizing A .

Proof. For any iteration r , A can be covered by a finite number of boxes of width w_r . This implies that a finite number of grid points discretize A , and hence, that some finite δ exists.

Suppose $\mathbf{x} \in \bar{B}^r$. By the definition of our grid, \mathbf{x} is contained in some $G = \text{Conv}(S)$, where S is a finite set of neighboring grid points. For each $\mathbf{x}_a, \mathbf{x}_b \in S$, $\mathbf{x}_b \in N(\mathbf{x}_a)$, and hence $c(\mathbf{x}_a, \mathbf{x}_b) \leq \delta$. Because \mathbf{x}_a and \mathbf{x}_b were arbitrarily chosen, this is true of every pair of vertices of G . By the definition of G , \mathbf{x} can be written as a convex combination of the points in S . Therefore, for any fixed $\mathbf{x}_0 \in S$, $c(\mathbf{x}, \mathbf{x}_0) \leq \delta$.

Because $\mathbf{x} \in \bar{B}^r$, $\text{Conv}(S) \cap B^r$ must be nonempty. Assume without loss of generality that $\mathbf{x}_0 = \mathbf{x}_i \in B_i^r$ for some $i \in \mathbb{N}_n$. By Theorem 3.19, there must exist a point $\mathbf{x}_j \in B_j^r$, a neighbor of \mathbf{x}_i , with $j \neq i$, and a point $\mathbf{b} \in A_{ij}$ such that $c(\mathbf{x}_i, \mathbf{b}) \leq c(\mathbf{x}_i, \mathbf{x}_j) \leq \delta$. Applying the triangle inequality, we find that

$$c(\mathbf{x}, \mathbf{b}) \leq c(\mathbf{x}, \mathbf{x}_i) + c(\mathbf{x}_i, \mathbf{b}) \leq 2\delta.$$

Therefore, $c(\mathbf{x}, B) \leq 2\delta$. □

3.3.4. Error bound for ground costs. In preparation for bounding the Wasserstein distance error, we now bound the error on the ground cost c with respect to individual points in \bar{B}^r .

Theorem 3.23. Let $\tilde{\pi}^*$ be an approximated transport plan consistent with the shift characterization and having associated transport map \tilde{T} . Suppose π^* is an optimal transport plan with associated map T , and let \mathbf{x} in A such that $T(\mathbf{x}) = \mathbf{y}_i$, but $\tilde{T}(\mathbf{x}) = \mathbf{y}_j$. Then the error in the ground cost at the point \mathbf{x} is equal to $|g_{ij}(\mathbf{x})|$. Furthermore, if c is a polynomial combination of ℓ_p functions with positive coefficients, then there exists γ_{\max} such that, for all $\mathbf{x} \in A$, if $T(\mathbf{x}) = \mathbf{y}_i$ and $\tilde{T}(\mathbf{x}) = \mathbf{y}_j$ for some $i \neq j$, then

$$|g_{ij}(\mathbf{x})| \leq \gamma_{\max} < \infty. \quad (3.17)$$

Proof. Let $\mathbf{x} \in A$ such that $T(\mathbf{x}) = \mathbf{y}_i$, but $\widetilde{T}(\mathbf{x}) = \mathbf{y}_j$. Then the error in the ground cost at \mathbf{x} equals

$$|c(\mathbf{x}, \mathbf{y}_i) - c(\mathbf{x}, \mathbf{y}_j)| = |g_{ij}(\mathbf{x})|.$$

Now suppose c is a polynomial combination of ℓ_p functions with positive coefficients, defined as described in Equation (3.14). Because all costs are nonnegative, and achieve their maximum with $c(0, l\mathbb{1}_d)$, for all $\mathbf{x} \in A$

$$|g_{ij}(\mathbf{x})| = |c(\mathbf{x}, \mathbf{y}_i) - c(\mathbf{x}, \mathbf{y}_j)| \leq c(0, l\mathbb{1}_d) = \sum_{s=1}^{\sigma} k_s \left(ld^{1/p_s} \right)^{q_s} < \infty. \quad \square$$

Lemma 3.24. *If c is a norm, then $\gamma_{\max} \leq \kappa_{\max} + 4\delta$, where*

$$\kappa_{\max} := \max_{\substack{1 \leq i < j \leq n \\ i < j \leq n}} |a_{ij}|, \quad (3.18)$$

and δ is the maximum ground cost for a pair of neighboring points in the grid discretizing A .

Proof. Let $\mathbf{x} \in \bar{B}^r$ and $i, j \in \mathbb{N}_n$ such that $i \neq j$. As a consequence of Theorems 3.17, 3.19, and 3.22:

$$|g_{ij}(\mathbf{x})| = |c(\mathbf{x}, \mathbf{y}_i) - c(\mathbf{x}, \mathbf{y}_j)| \leq |a_{ij}| + |\alpha_{ij}(\mathbf{x})| \leq \kappa_{\max} + 2c(\mathbf{x}, \mathbf{b}) \leq \kappa_{\max} + 4\delta.$$

Because the result is independent of \mathbf{x} , i , and j , $\gamma_{\max} \leq \kappa_{\max} + 4\delta$. \square

3.3.5. Volume and containment for the boundary region. As shown in Section 3.3.4, the ground cost error for individual points is finitely bounded over a wide range of admissible ground cost functions. By definition, the measure μ is bounded. We propose to identify the largest possible region in which the ground cost error can be non-zero, and to show that the area of that region goes to zero as r goes to infinity. With this, we will show that the boundary method converges with respect to the Wasserstein distance.

In Equation (3.12), we defined a region \bar{B}^r based on the point set B^r . For this, we need to know that we can choose an initial width w_1 such that, for all iterations r , $B \subset \bar{B}^r$. Fortunately, we can discretize A with respect to the Lebesgue measure and Euclidean distance in \mathbb{R}^d .

Theorem 3.25. *There exists an initial width w_1 such that, for all w_r such that $w_r \leq w_1$, $\mathbf{x} \in \mathring{A}_i^r$ implies $\mathbf{x}^r \subseteq \mathring{A}_i$, the strict interior of A_i , as defined by Equation (2.3).*

Proof. Assume the contrary and consider what happens as the region volumes go to zero. Given our initial assumptions, for the theorem to be false, we must have some point $\mathbf{p} \in A_i$, surrounded by an open hollow sphere in A_j of radius $\delta > 0$. Let the hollow sphere be given by

$$S := \{\mathbf{x} \in X \setminus \{\mathbf{p}\} \mid \|\mathbf{x} - \mathbf{p}\|_2 < \delta\} \subset A_j.$$

By the continuity of F , we have $\mathbf{p} \in A_{ij}$. Thus, \mathbf{p} is a point on the level set $g_{ij}(\mathbf{x}) = a_i - a_j$. Define

$$S_g := S \setminus \{\mathbf{x} \in A \mid g_{ij}(\mathbf{x}) = a_i - a_j\}.$$

S_g is the union of two disjoint, nonempty open sets

$$S^+ := \{\mathbf{x} \in S \mid g_{ij}(\mathbf{x}) > a_i - a_j\}$$

and

$$S^- := \{\mathbf{x} \in S \mid g_{ij}(\mathbf{x}) < a_i - a_j\}.$$

However, for all \mathbf{x} in the nonempty set S^- , $a_j - c(\mathbf{x}, \mathbf{y}_j) < a_i - c(\mathbf{x}, \mathbf{y}_i)$, and therefore $\mathbf{x} \notin A_j$. This contradicts that S is a subset of A_j . \square

Next, we show that it is possible to choose an initial width and grid arrangement to guarantee that each point in $A^r \setminus B^r$ corresponds to a box in the interior of some region A_i .

Theorem 3.26. *Suppose w_1 is chosen as described in Theorem 3.25. Fix r , and let $w_r \leq w_1$. If $B \subseteq \bar{A}^r$, then $B \subseteq \bar{B}^r$, and hence $B \subseteq A^{r+1}$.*

Proof. We will show the conclusions by proving that $\mathbf{x}_0 \notin \bar{B}^r$ implies $\mathbf{x}_0 \notin B$.

Suppose $\mathbf{x}_0 \notin \bar{B}^r$. If $\mathbf{x}_0 \notin \bar{A}^r$, then $\mathbf{x}_0 \notin B$, since by assumption, $B \subseteq \bar{A}^r$. Thus, we assume instead that $\mathbf{x}_0 \in \bar{A}^r \setminus \bar{B}^r$.

Because $\mathbf{x}_0 \in \bar{A}^r$, we know $\mathbf{x}_0 \in \mathbf{x}^r$ for some $\mathbf{x} \in A^r$. We have $\mathbf{x} \in A_i$ for some $i \in \mathbb{N}_n$, and so $\mathbf{x} \in \bar{A}_i^r$. However, $\mathbf{x}_0 \notin \bar{B}^r$ implies $\mathbf{x}^r \not\subseteq \bar{B}^r$, so $\mathbf{x} \notin B^r$. Because, $\mathbf{x} \in \bar{A}_i^r \setminus B^r = \mathring{A}_i^r$, by Theorem 3.25, $\mathbf{x}^r \subseteq \mathring{A}_i$. Hence, $\mathbf{x}_0 \in \mathring{A}_i$. Therefore, by Equation (2.3), $\mathbf{x}_0 \notin B$. \square

Now that we have ensured $B \subseteq \bar{B}^r$, we aim to construct a region of controlled volume enclosing \bar{B}^r : $\bar{B}^r \subseteq \bar{B}_+^r$. Then we show that, as $r \rightarrow \infty$, the volume of \bar{B}_+^r in \mathbb{R}^d goes to zero with respect to the Lebesgue measure. This will allow us to put a convenient upper bound on the volume of \bar{B}^r in terms of the width w_r . Because \bar{B}_+^r exists solely in A , and not on the product space, we can once again rely on the Euclidean distance in \mathbb{R}^d .

Theorem 3.27. *Let the region $\bar{B}_+^r \subseteq A$ be defined as*

$$\bar{B}_+^r := \{\mathbf{x} \in A \mid \|\mathbf{x} - B\|_2 \leq 2w_r\sqrt{d}\}. \quad (3.19)$$

For all r , $\bar{B}^r \subseteq \bar{B}_+^r$.

Proof. By definition, $\bar{B}^r \subseteq A$. Suppose $x \in \bar{B}^r$. Because we are applying the Euclidean norm, by Theorem 3.22, we know that $\|\mathbf{x} - B\|_2 \leq 2\delta$. Let \mathbf{x}_0 and $\mathbf{x}_1 \in N(\mathbf{x}_0)$ be elements of the r -th discretization grid of the set A . By the definition of neighbors, we can write $\mathbf{x}_1 = \mathbf{x}_0 + w_r\mathbf{v}$ for some $\mathbf{v} \in \mathcal{V}$. Thus,

$$\|\mathbf{x}_1 - \mathbf{x}_0\|_2 = w_r\|\mathbf{v}\|_2 \leq w_r\sqrt{d}.$$

Because \mathbf{x}_0 and \mathbf{x}_1 were arbitrarily chosen, this is true of every pair of neighbors. This implies $\delta \leq w_r\sqrt{d}$. Therefore, $\|\mathbf{x} - B\|_2 \leq 2w_r\sqrt{d}$, and since $\mathbf{x} \in A$, $\mathbf{x} \in \bar{B}_+^r$. \square

Theorem 3.28. *If $|B| = \tilde{L} < \infty$ with respect to the \mathbb{R}^{d-1} Lebesgue measure, then there exists some $L < \infty$, such that $|\bar{B}^r| \leq w_r^d L$ with respect to the \mathbb{R}^d Lebesgue measure.*

Proof. Assume that $|B| = \tilde{L} < \infty$. We know $\int_{\bar{B}_+^r} d\mathbf{x} = \int_A \chi[\bar{B}_+^r](\mathbf{x}) d\mathbf{x}$. Let $\mathcal{B}(\mathbf{x}, \rho)$ be the closed ball of radius ρ centered at \mathbf{x} , and write

$$\begin{aligned} \int_A \chi[\bar{B}_+^r](\mathbf{x}) d\mathbf{x} &= \int_A \chi\left[\left\{\mathbf{x} \in A \mid \|\mathbf{x} - B\|_2 \leq 2w_r\sqrt{d}\right\}\right](\mathbf{x}) d\mathbf{x} \\ &= \int_A \chi\left[\left\{\mathbf{x} \in A \mid \mathbf{x} \in \mathcal{B}(\mathbf{z}, 2w_r\sqrt{d}) \text{ for some } \mathbf{z} \in B\right\}\right](\mathbf{x}) d\mathbf{x}, \\ &\leq \int_A \chi[B](\mathbf{z}) \left(\int_A \chi[\mathcal{B}(\mathbf{z}, 2w_r\sqrt{d})](\mathbf{x}) d\mathbf{x}\right) d\mathbf{z}. \end{aligned}$$

For all fixed \mathbf{x} ,

$$\int_A \chi[\mathcal{B}(\mathbf{x}, 2w_r\sqrt{d})](\mathbf{x}) d\mathbf{x} \leq \text{Vol}_d(2w_r\sqrt{d}),$$

where $\text{Vol}_d(\rho)$ is the volume of the d -dimensional sphere of radius ρ . By using the Γ function, this volume can be written as

$$\begin{aligned} \text{Vol}_d(2w_r\sqrt{d}) &:= \frac{\pi^{d/2}}{2\Gamma(\frac{d}{2})} (2w_r\sqrt{d})^d \\ &= \begin{cases} \frac{\pi^{d/2}}{(d/2)!} (2w_r\sqrt{d})^d & \text{if } d = 2k \text{ for some } k \in \mathbb{Z} \\ \frac{2k!(4\pi)^k}{d!} (2w_r\sqrt{d})^d & \text{if } d = 2k + 1 \text{ for some } k \in \mathbb{Z}. \end{cases} \end{aligned}$$

Because the volume is independent of the point $\mathbf{x} \in A$, we therefore have

$$\begin{aligned} \int_{\bar{B}_+^r} d\mathbf{x} &\leq \int_A \chi[B](\mathbf{z}) \int_A \chi[\mathcal{B}(\mathbf{z}, 2w_r\sqrt{d})](\mathbf{x}) d\mathbf{x} d\mathbf{z}, \\ &\leq \int_A \chi[B](\mathbf{z}) \text{Vol}_d(2w_r\sqrt{d}) d\mathbf{z} = \text{Vol}_d(2w_r\sqrt{d}) \int_B d\mathbf{z} = w_r^d L, \end{aligned}$$

where

$$L := \begin{cases} \tilde{L} \frac{\pi^{d/2}}{(d/2)!} (2\sqrt{d})^d & \text{if } d = 2k \text{ for some } k \in \mathbb{Z} \\ \tilde{L} \frac{2k!(4\pi)^k}{d!} (2\sqrt{d})^d & \text{if } d = 2k + 1 \text{ for some } k \in \mathbb{Z}. \end{cases}$$

Let $\mathbf{x} \in \bar{B}^r$. Because $\|\cdot\|_2$ is a norm, by applying Theorem 3.22 with $c = \ell_2$, we know that for all $\mathbf{x} \in \bar{B}^r$, $\|\mathbf{x} - B\|_2 \leq 2\delta$. For our box grid of width w_r , $\delta = w_r\sqrt{d}$ when $c = \ell_2$. Hence, $\|\mathbf{x} - B\|_2 \leq 2w_r\sqrt{d}$, which implies $\mathbf{x} \in \bar{B}_+^r$. Thus, $\bar{B}^r \subseteq \bar{B}_+^r$, which implies $|\bar{B}^r| \leq |\bar{B}_+^r| \leq w_r^d L$. \square

Remark 3.29. The interplay between B , B^r , \bar{B}^r , and \bar{B}_+^r is nontrivial. Figure 3 helps to visualize it properly. In Figure 3(a), we show placement of some boundary set B^r . It is crucial that the subgrid created by B^r completely surrounds B , because that is the only way to ensure that $B \subseteq \bar{B}^r$. One can see in this image how a (very degenerate) choice of c , coupled with the right arrangement of \mathbf{y}_i 's, might allow a small and sharply curved boundary set to slip unnoticed between points.

As Figure 3(b) illustrates, each point in B^r appears as the center of its corresponding box, and the boxes completely cover the boundary set.

The region \bar{B}_+^r is deliberately constructed to entirely cover all the boxes in \bar{B}^r . As Figure 3(c) shows, its volume can be significantly larger than that of the boxes it contains. However, the worst-case ‘‘thickness’’ given to \bar{B}_+^r ensures that it will always enclose both B and \bar{B}^r .

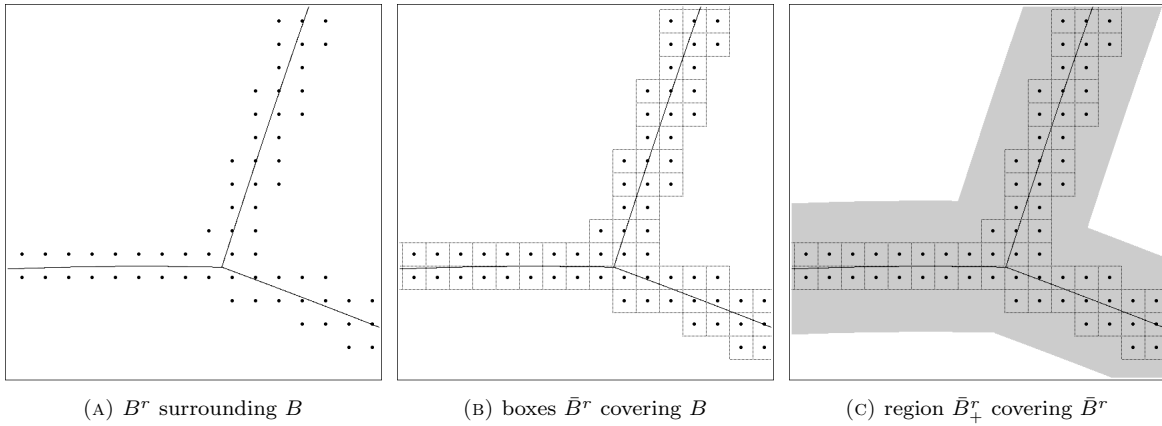


FIGURE 3. Detail from problem in Figure 5(a): Boundary set interactions near $A_0 \cap A_2 \cap A_3$

3.3.6. The Wasserstein distance error.

Theorem 3.30. *Let P^* be the Wasserstein distance and let M be the maximum value of μ on A . Suppose $B \subseteq \bar{B}^r$, and that there exists some L such that $|\bar{B}^r| = w_r^d L < \infty$ with respect to the d -dimensional Lebesgue measure. If $\gamma_{\max} < \infty$ is the maximum error of the ground cost in the set \bar{B}^r , and \tilde{P}^* is the Wasserstein distance approximation obtained with the boundary method, then:*

$$\left| \tilde{P}^* - P^* \right| \leq w_r^d L M \gamma_{\max}, \quad (3.20)$$

where the bound equals the maximum possible volume of \bar{B}^r multiplied by the maximum value of μ and the maximum error of the ground cost.

Proof. If $\mathbf{x} \in A \setminus \bar{B}^r$, then \mathbf{x} has been identified as being in the interior of A_i for some $i \in \mathbb{N}_n$. Thus, the cost error associated with the points outside \bar{B}^r is zero.

Suppose instead that $\mathbf{x} \in \bar{B}^r$. By definition, the absolute value of the difference between the correct and approximated ground costs at \mathbf{x} is less than or equal to γ_{\max} .

Therefore, the error on the Wasserstein distance is bounded above by

$$\begin{aligned} \left| \tilde{P}^* - P^* \right| &\leq \int_{\bar{B}^r} \gamma_{\max} d\mu(\mathbf{x}) = \int_{\bar{B}^r} \mu(\mathbf{x}) \gamma_{\max} d\mathbf{x} \\ &\leq \int_{\bar{B}^r} (M) \gamma_{\max} d\mathbf{x} = |\bar{B}^r| M \gamma_{\max} \leq (w_r L) M \gamma_{\max}. \end{aligned} \quad \square$$

Remark 3.31. The bounds in Theorems 3.28 and 3.30 indicate that the approximation error in computing the boundary set and the Wasserstein distance decreases linearly with the volume of the boxes. When

Theorem 3.28 applies, we expect a quadratic (in \mathbb{R}^2) or cubic (in \mathbb{R}^3) decrease of the error. These decreases are clearly observed in practice, see Section 5.

4. TEST CONDITIONS

As mentioned in Remark 2.1, certain choices of μ may make it necessary to approximate $\mu(\mathbf{x}^r)$ or $\int_{\mathbf{x}^r} c(\mathbf{z}, \mathbf{y}_i) d\mu(\mathbf{z})$. However, the majority of numerical studies we have seen restrict to simple choices of μ (most often uniform). For this reason, we restricted our examples to cases where the cost and mass integrals can be written in a closed form.

4.1. **The closed-form mass $\mu(\mathbf{x}^r)$.** The integral of μ over some box can be written as:

$$\mu(\mathbf{x}^r) = \int_{\mathbf{x}^r} \mu(\mathbf{z}) d\mathbf{z} = M(\mathbf{z}) \Big|_{\mathbf{z} \in \mathbf{x}^r} \quad \text{with} \quad M : X \rightarrow \mathbb{R}^{\geq 0}. \quad (4.1)$$

Since μ is a probability density function, we must have $\int_A d\mu = 1$. For convenience, let $\hat{\mu}$ denote an unnormalized version of μ , and similarly for \hat{M} .

Using the linearity of the integral, one can use linear combination of simple functions for which exact solutions are known. We can also construct more complex measures by partitioning A into disjoint subsets. In this case, however, we add an additional restriction in order to be sure that exact solutions can always be found: We μ -partition A into subsets S_1, \dots, S_σ , such that the boundaries of each S_s fall on the initial set of grid lines. Assume that for each set S_s , there exists a density function $\hat{\mu}_s$ that is exactly solvable on S_s . From these, we consider $\hat{\mu}$ (and \hat{M}) to be the piecewise functions defined on each S_s as $\hat{\mu}_s$ (and \hat{M}_s , respectively).

Most of our computations were performed in two-dimensions. For such problems, given iteration r and $\mathbf{x} = (x_1, x_2) \in A$, $\hat{\mu}(\mathbf{x}^r)$ can be written as

$$(4.2) \quad \begin{aligned} \hat{\mu}(\mathbf{x}^r) = & \hat{M}(x_1 + w_r/2, x_2 + w_r/2) - \hat{M}(x_1 + w_r/2, x_2 - w_r/2) \\ & - \hat{M}(x_1 - w_r/2, x_2 + w_r/2) + \hat{M}(x_1 - w_r/2, x_2 - w_r/2). \end{aligned}$$

The closed-form choices used in our numerical tests are shown in Table 1. As described above, we used the table entries as building blocks in the construction of more complex measures.

TABLE 1. Closed-form options for μ

$\hat{\mu}((x_1, x_2)) = 1$		$\hat{M}(u, v) = uv$
$\hat{\mu}((x_1, x_2)) = x_1^t x_2^t,$	$t > 0$	$\hat{M}(u, v) = (t+1)^{-2} (u^{t+1} v^{t+1})$
$\hat{\mu}((x_1, x_2)) = e^{tx_1},$	$t \neq 0$	$\hat{M}(u, v) = t^{-1} v e^{tu}$
$\hat{\mu}((x_1, x_2)) = e^{tx_2},$	$t \neq 0$	$\hat{M}(u, v) = t^{-1} u e^{tv}$

4.2. **The closed-form Wasserstein distance over \mathbf{x}^r .** We performed many tests where μ could be computed exactly but the Wasserstein distance could not; see Section 5 for details. In such cases, we made no attempt to approximate P^* , choosing instead to focus on the accuracy of the μ -partition generated by the approximate shift set $\{\tilde{a}_i\}_{i=1}^n$.

However, there were a number of cases in two dimensions where the choice of μ and c allowed for closed-form computations. In those cases, because the combination of c and μ gives us an exact solution, there exists $C : X \times Y \rightarrow \mathbb{R}^{\geq 0}$ such that

$$\int_{\mathbf{x}^r} c(\mathbf{z}, \mathbf{y}_i) d\mu(\mathbf{z}) = C(\mathbf{z}, \mathbf{y}_i) \Big|_{\mathbf{z} \in \mathbf{x}^r}. \quad (4.3)$$

As in Section 4.1, we write \hat{C} when working with $\hat{\mu}$.

Now consider $X, Y \subset \mathbb{R}^2$, $\mathbf{x} = (x_1, x_2) \in A$, and $\mathbf{y} = (y_1, y_2) \in \{\mathbf{y}_i\}_{i=1}^n$. When $\mu(\mathbf{x}^r) = 0$, the Wasserstein distance on \mathbf{x}^r is also zero. For those boxes where $\mu(\mathbf{x}^r) > 0$, we can take advantage of the uniformity to define the function \hat{C} in terms of a single variable: the component-wise distance between points given by

(Δ_1, Δ_2) , where $\Delta_1 = |x_1 - y_1|$, $\Delta_2 = |x_2 - y_2|$. When the Wasserstein distance over \mathbf{x}^r can be computed and is non-zero, it takes the form

$$(4.4) \quad \int_{\mathbf{x}^r} c(\mathbf{z}, \mathbf{y}) d\hat{\mu}(\mathbf{z}) = \hat{C}(\Delta_1 + w_r/2, \Delta_2 + w_r/2) - \hat{C}(\Delta_1 + w_r/2, \Delta_2 - w_r/2) \\ - \hat{C}(\Delta_1 - w_r/2, \Delta_2 + w_r/2) + \hat{C}(\Delta_1 - w_r/2, \Delta_2 - w_r/2),$$

where $\hat{C} : \mathbb{R}^2 \rightarrow \mathbb{R}^{\geq 0}$ is an explicit function.

Table 2 gives Wasserstein distance functions \hat{C} for $c = \ell_2$ and all $c = \ell_p^p$ with $p > 0$. By leveraging the linearity of the integral and subdividing A into disjoint sets, we can build combinations of ground costs and measures with closed form C . We used this to perform tests in \mathbb{R}^2 , with μ being either uniform or zero in relevant boxes.

TABLE 2. Closed-form options for C when μ is uniform or zero on A

c	$\hat{C}(u, v)$
ℓ_2	$\begin{cases} \frac{1}{6}u^3 \log(\sqrt{u^2 + v^2} + v) \\ \quad + \frac{1}{3}uv\sqrt{u^2 + v^2} \\ \quad + \frac{1}{6}v^3 \log(\sqrt{u^2 + v^2} + u) & \text{if } (u, v) \neq \mathbf{0} \\ 0 & \text{if } (u, v) = \mathbf{0} \end{cases}$
$\ell_p^p, \quad p > 0$	$(p+1)^{-1}(u^{p+1}v + uv^{p+1})$

5. NUMERICAL RESULTS

5.1. Accuracy of the Wasserstein distance.

5.1.1. *When exact values are known.* When μ is uniform, we use the formula for $c = \ell_2$, given in Table 2, to compute exact values for the two problems shown in Figure 4.

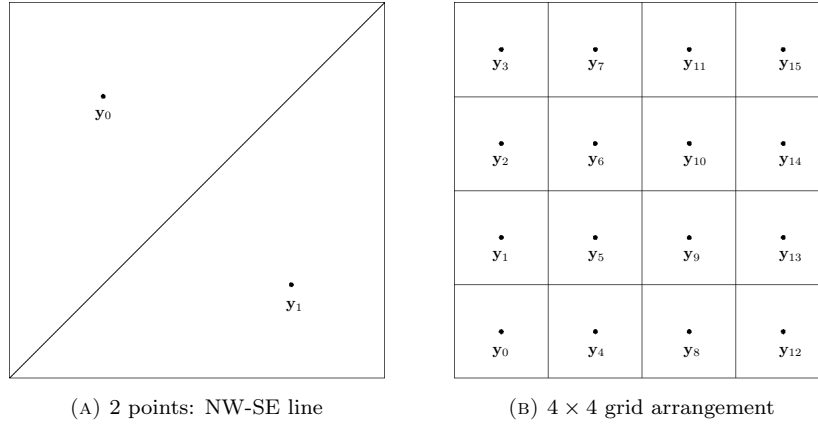


FIGURE 4. Problems where the exact Wasserstein distance and set of shifts are known

For two points on the Northwest-Southeast diagonal, placed as shown in Figure 4(a), the exact Wasserstein distance is equal to

$$P_{\text{NWSE}}^* := \frac{1}{96} \left[\sqrt{2} + 7\sqrt{10} + \sinh^{-1}(1) + 2\sqrt{2} \sinh^{-1}(2) + \sinh^{-1}(3) \right] \\ \approx 0.3159707808963017.$$

Table 3(a) shows the error. Note that the actual decrease in error is roughly quadratic in w_* : $|\tilde{P}^* - P^*| \approx 2.122(w_*)^{1.995}$.

TABLE 3. Wasserstein errors for the NWSE and 4×4 problems

w_*	abs. error	w_*	abs. error
2^{-9}	8.42×10^{-6}	2^{-9}	2.02×10^{-5}
2^{-10}	2.11×10^{-6}	2^{-10}	5.04×10^{-6}
2^{-11}	5.27×10^{-7}	2^{-11}	1.26×10^{-6}
2^{-12}	1.32×10^{-7}	2^{-12}	3.15×10^{-7}
2^{-13}	3.30×10^{-8}	2^{-13}	7.88×10^{-8}
2^{-14}	8.24×10^{-9}	2^{-14}	1.97×10^{-8}
2^{-15}	2.06×10^{-9}	2^{-15}	4.93×10^{-9}
2^{-16}	5.15×10^{-10}	2^{-16}	1.23×10^{-9}
2^{-17}	1.29×10^{-10}	2^{-17}	3.08×10^{-10}

(A) NWSE errors (B) 4×4 errors

When we have a 4×4 arrangement of boxes, with each \mathbf{y}_i in the center, as shown in Figure 4(b), the exact Wasserstein distance is equal to

$$P_{4 \times 4}^* := \frac{1}{24} \left[\sqrt{2} + \sinh^{-1}(1) \right] \approx 0.09564946455802659. \quad (5.1)$$

Table 3(b) shows the absolute error for various choices of w_* . Again, the observed error decrease is roughly quadratic in w_* : $|\tilde{P}^* - P^*| \approx 5.254(w_*)^{1.999}$.

For both problems, we also know the exact shift values: since every point in A goes to the nearest \mathbf{y}_i , the shift differences are all zero, which means every shift must be identical. In the 4×4 problem, the shift values are identical for every choice of w_* . This is a result of computing regions that exactly correspond to the structure of our grid. The shift values for the NWSE problem show that the decrease in shift error is roughly linear with respect to w_* : $|\tilde{a}_2 - \tilde{a}_1| \approx 0.339(w_*)^{1.008}$. When $w_* = 2^{-16}$, the shift error is about 4.83×10^{-6} .

5.1.2. *When exact values are not known.* As Section 3.3.6 shows, even if the Wasserstein distance is unknown, the Wasserstein approximation error at the end of the r -th iteration is bounded above by

$$\sum_{\mathbf{x} \in B^r} \mu(\mathbf{x}^r) \max_{\mathbf{x}_0 \in \mathbf{x}^r} g_{ij}(\mathbf{x}_0), \quad (5.2)$$

where i and j , $i \neq j$ refer to the destinations of \mathbf{x} and some neighbor.

As $w_r \rightarrow 0$, $\max_{\mathbf{x}_0 \in \mathbf{x}^r} g_{ij}(\mathbf{x}_0) \rightarrow |a_{ij}|$ for each $i \neq j$, and $\mu(\bar{B}^r) \rightarrow 0$. Hence, if the boundary method is working effectively, at worst we can expect to see these error values decreasing linearly with respect to $\mu(\bar{B}^r)$.

We considered the change in the approximated Wasserstein distance for Example 2.2 using three canonical ℓ_p ground costs: ℓ_1 , ℓ_2 , and ℓ_2^2 . The resulting μ -partitions are shown in Figures 7(a), 5(a), and 8(a), respectively.

For each ground cost, we computed the Wasserstein approximation error in two ways:

- (1) The worst-case error bound given by applying (5.2).
- (2) The rate of change with respect to a reference approximation,

$$\Delta \tilde{P}_{16}^*(w_*) := \Delta \tilde{P}_{16}^*(2^{-m}) = \frac{|\tilde{P}_m^* - \tilde{P}_{16}^*|}{|\tilde{P}_{m+1}^* - \tilde{P}_{16}^*|}, \quad \text{for } m < 15.$$

In all three cases, the worst-case error is roughly linear in w_* , and the rate of change $\Delta \tilde{P}_{16}^*$ is roughly quadratic in w_* . Specific results are given in Table 4.

5.2. μ -Partitions in \mathbb{R}^2 .

TABLE 4. Wasserstein approximation behavior with respect to w_*

c	\tilde{P}_{16}^*	$\text{err}_{\max}(w_*)$	$\Delta \tilde{P}_{16}^*(w_*)$
ℓ_1	0.25702262181	$0.457(w_*)^{1.020}$	$1.186(w_*)^{2.025}$
ℓ_2	0.20754605961	$0.361(w_*)^{1.008}$	$4.151(w_*)^{2.023}$
ℓ_2^2	0.05290682486	$0.221(w_*)^{1.008}$	$2.668(w_*)^{2.029}$

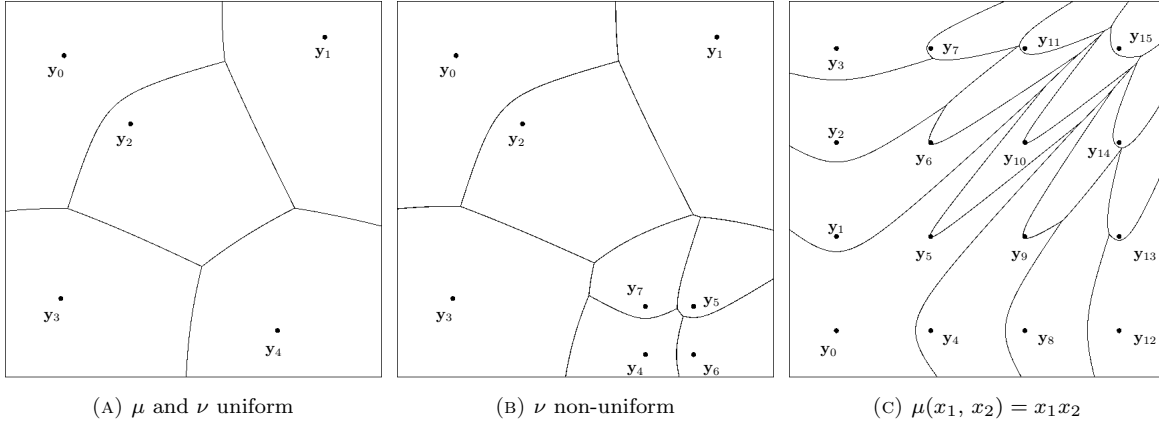


FIGURE 5. Partitions for uniform and non-uniform measures

5.2.1. *Uniform and non-uniform measures μ and ν .* We include three examples of variations on μ and ν , shown in Figure 5. All three assume c is the Euclidean distance.

In Figure 5(a), we assume μ is the uniform continuous probability distribution on A , and ν is the uniform discrete distribution with $n = 5$. The five points where $\nu = 1/5$ are placed in the positions used in [1]. Figure 5(a) shows the μ -partition obtained by the boundary method; for comparison, see [1, Figure 3 (right)].

Starting from the points shown in Figure 5(a), we next take the point \mathbf{y}_4 and split it into four new points, each of one quarter-mass, positioned equidistantly from the point's original location. This gives us a non-uniform ν with four points of weight $1/5$ and four of weight $1/20$. We keep μ uniform. The resulting μ -partition is shown in Figure 5(b).

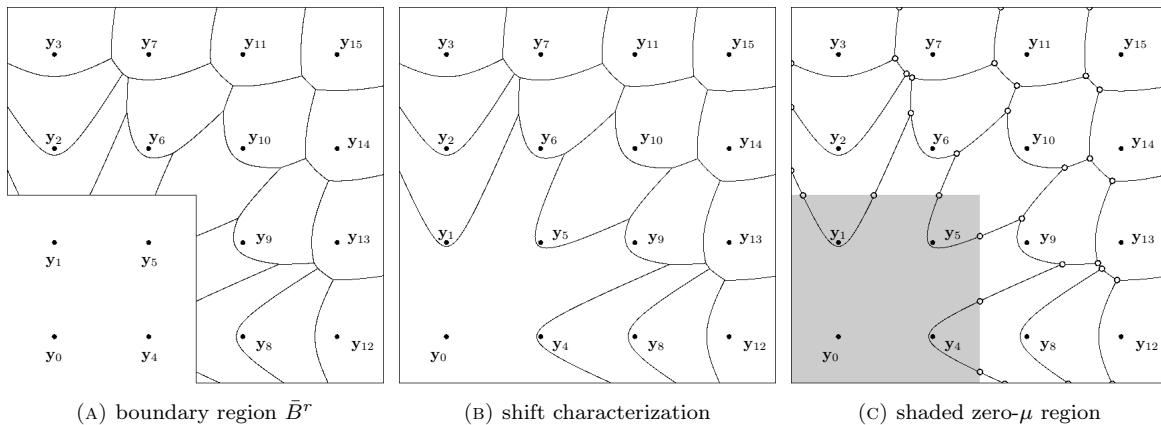
In Figure 5(c), we choose the nonuniform probability density $\mu(x_1, x_2) = \frac{1}{4}x_1x_2$. For ν , we choose the uniform 4×4 grid of points given in Figure 4(b). By comparing the results in Figures 4(b) and 5(c), the impact of μ 's nonuniformity becomes obvious. While the individual regions no longer have equal Lebesgue measure, each has equal μ -measure $1/16$. The larger regions in the lower-left correspond to the lower density of μ in that corner, while the smaller regions in the upper-right correspond to the higher concentration of μ -density there.

5.2.2. *Discontinuous and zero-measure μ .* Next, we deliberately introduce a discontinuous μ that is not strictly positive:

$$\mu(\mathbf{x}) = \begin{cases} 0 & \text{if } \mathbf{x} \in [0, 1/2]^2 \\ 4/3 & \text{otherwise.} \end{cases} \quad (5.3)$$

We still have $\int_A d\mu(\mathbf{x}) = 1$, so μ is a probability density function on $A = [0, 1]^2$. For ν , we use the same uniform 4×4 grid shown in Figure 4(b).

Figure 6 shows the results. In Figure 6(a), we see the boundary set used to generate the solution. Points between regions are retained, as are points adjacent to regions of measure zero. No computations are done on the lower-left region, because any destination is equally valid on boxes of μ -measure zero.

FIGURE 6. μ is zero in the lower-left quadrant

However, when the shift definition is applied to the semi-discrete optimal transport problem, there is only one valid shift-characterized solution over A . Figure 6(b) shows that solution. The unique shift differences force the selection of a unique boundary set B , even in the region where μ is zero.

Figure 6(c) shows the shift characterization again, but here the region of μ -zero measure is shaded, helping to confirm visually that the regions have equal measure. Figure 6(c) also shows the locations of intersection points we identified using the boundary method.

5.2.3. Norms as ground cost functions. The computations in Sections 5.2.1 and 5.2.2 all assume the ground cost function equals the Euclidean distance. In fact, we can apply the boundary method to a wide range of polynomial ℓ_p ground costs. Using the same problem solved with the Euclidean distance in Figure 5(a), we generated μ -partitions for a wide range of ℓ_p -norm ground costs. Results for the ℓ_1 , ℓ_{10} , and ℓ_∞ norms are shown in Figure 7.

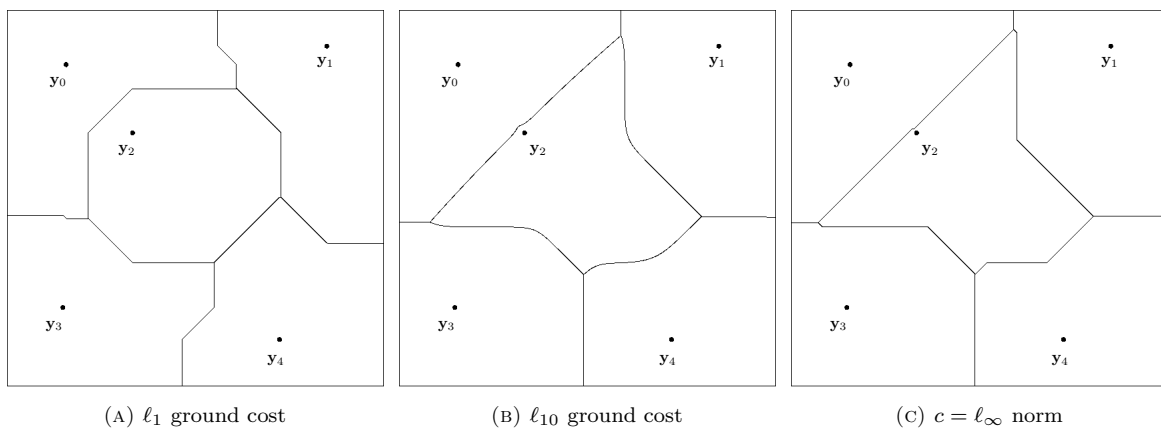


FIGURE 7. Equal area using different ground cost norms

5.2.4. Other ground costs c . The computations above all assume that the ground cost function is a norm. However, the boundary method works equally well on much more general ground cost functions. Three examples are shown in Figure 8.

Figure 8(a) shows the result given by ℓ_2^2 . Because ℓ_2^2 is not a norm, we were only able to make the most general mathematical claims regarding its behavior. However, the boundary method has no trouble with it. In fact, its convergence behavior is practically identical to that of the norms ℓ_1 and ℓ_2 .

As Figure 8(b) illustrates, even ℓ_p costs with $p < 1$ can be approximated; when $p < 1$, the regions become discontinuous, as typified by the “spikes” on the exterior walls. (The spike on the lower right is part of

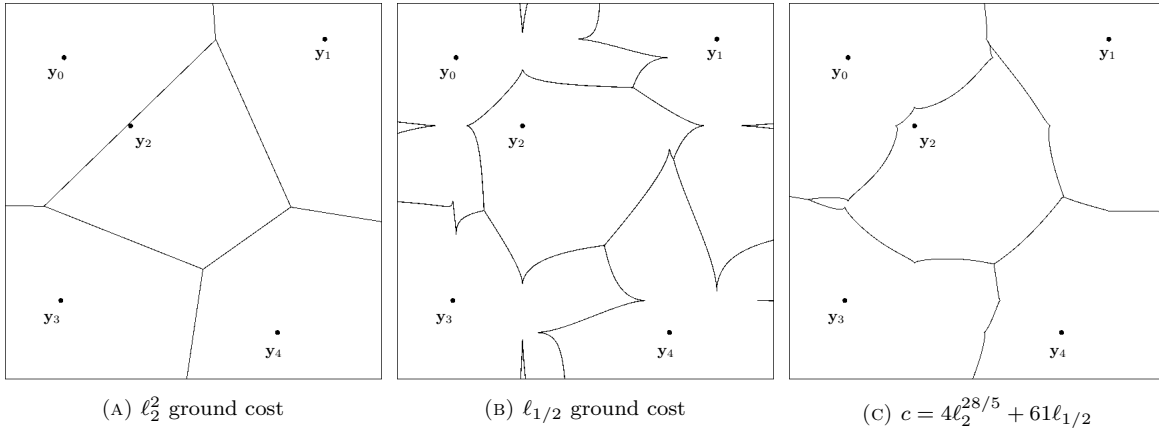
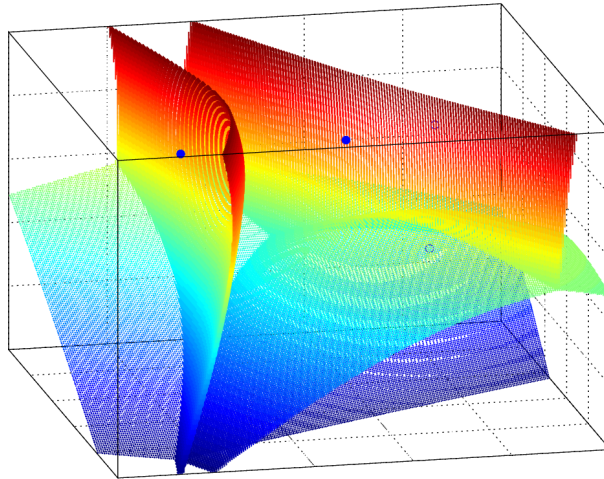


FIGURE 8. Equal area using non-norm ground costs

the region coupled with \mathbf{y}_3 , while the other four spikes are coupled with \mathbf{y}_2 .) Note that $\ell_{1/2}$ is a concave function. Such functions are directly applicable to transport problems involving economies of scale; e.g., see [12]).

Figure 8(c) shows a ground cost function defined as a polynomial combination of ℓ_p functions with positive coefficients: $c = 4\ell_2^{28/5} + 61\ell_{1/2}$. This function is neither convex nor concave, changing behavior with distance.

5.3. μ -Partitions in \mathbb{R}^3 . As we showed in Section 3, there is no theoretical obstacle to applying the boundary method to higher-dimensional problems, though of course visualization is complex.

FIGURE 9. Three-dimensional semi-discrete solution with $n = 5$

The image in Figure 9 was generated by taking $c = \ell_2$, μ the uniform continuous probability density, and ν the uniform discrete probability density with five randomly-placed non-zero points in $[0, 1]^3$. Even in this relatively simple case, it is impossible to find a single point-of-view that clearly shows all five non-zero points while clearly illustrating the boundaries of the μ -partitions. However, even though clear illustration is problematic, the computations made with the boundary method were completely successful.

5.4. Scaling behavior. One important advantage to the boundary method is its reduction of the complexity of the discretized problem, compared to traditional methods. Before considering the numerical results, it is worth developing a generalized comparison that puts this reduction in perspective:

Suppose for the sake of argument that a discretization with width 2^{-M} is required to solve a problem in \mathbb{R}^2 with N positive points in Y . Generating the full grid would create a product space $X \times Y$ of size $2^{2M}N$.

Say the boundary method is used instead, with a fixed initial discretization width of 2^{-4} . Each application of Step (2) of the boundary method algorithm removes approximately half the points in A^r , so by discarding interiors the method constructs a product space of size $2^{M+4}N$.

Assume that we compute solutions for both the boundary method and the full product space using the same linear solver (e.g., the network simplex method). Using it to solve the largest boundary problem of size $2^{M+4}N$, we have $V = 2^{M+4} + N$ vertices and $E = 2^{M+4}N$ edges. Solving over the full product space gives $V = 2^{2M} + N$ vertices and $E = 2^{2M}N$ edges. Hence, even if we assumed a solver with complexity $\mathcal{O}(V)$ (and no such solver exists), the ratio would be approximately 2^M to M . Typically, it is closer to 2^{2M} to M .

Of course, this improved complexity would be irrelevant if the constant factor was excessively large. Fortunately, that this is not the case, as our next section illustrates.

5.4.1. *Scaling on the plane with respect to $W = 1/w_*$.* Here we consider scaling on the plane with respect to $W = \frac{1}{w_*}$. We used Example 2.2, with μ and ν be uniform and $c = \ell_2$. The locations of the 5 points where $\nu = 1/5$ were fixed as depicted in Figure 5(a). We defined target widths $w_* = 2^{-m}$, $m \in \mathbb{N}$, and computed the time taken by the boundary method. By repeating this process for a few different location sets (and averaging them), we estimated the average scaling behavior of the boundary method with respect to W . The test results are shown in Table 5(a), and the scaling equations are on the left side of Table 6.

TABLE 5. Planar scaling with respect to W and N

$N = 5$			$W = 2^{10}$			$W = 2^{11}$	
W	T (sec)	S (MB)	N	T (sec)	S (MB)	T (sec)	S (MB)
2^{12}	0.855	24.540	128	6.938	17.25	22.365	33.91
2^{13}	2.005	49.100	136	12.190	18.24	36.601	35.05
2^{14}	4.497	98.210	144	10.982	17.99	29.952	36.49
2^{15}	11.025	196.400	152	13.139	18.54	36.703	41.27
2^{16}	28.093	394.400	160	11.420	18.66	34.801	40.27
2^{17}	60.577	785.800	168	15.727	20.97	44.959	40.66
2^{18}	132.397	1571.840	176	15.332	21.38	44.873	43.06
2^{19}	292.158	3151.872	184	18.243	21.38	53.689	43.20
2^{20}	640.660	6309.888	192	12.796	21.60	40.029	43.66

(A) Scaling with W

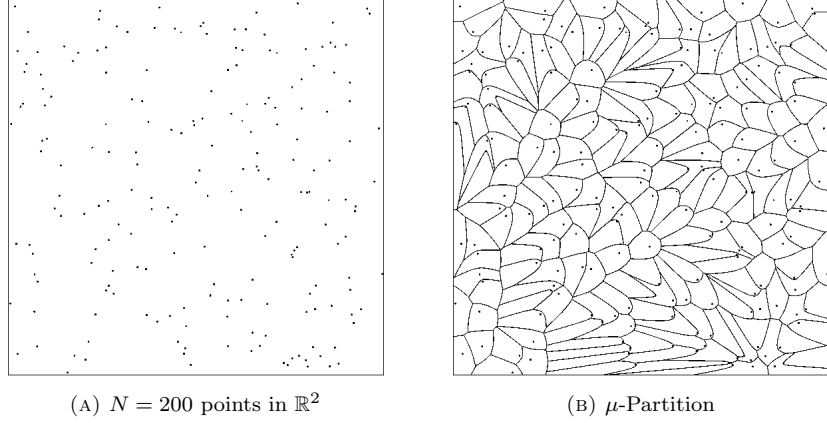
(B) Scaling with respect to N

TABLE 6. Time and storage scaling with respect to W and N separately

$T(W) \approx 4.356 \times 10^{-5} W \ln W$	Time	$T(N) \approx 4.582 \times 10^{-2} N \ln N$
$S(W) \approx 6.015 \times 10^{-3} W$	Storage	$S(N) \approx 3.162 N^{1/2}$

5.4.2. *Scaling on the plane with respect to N .* To evaluate planar scaling with respect to N , we performed multiple runs in $[0, 1]^2$ where $W = 2^{11}$ was fixed and μ and ν were uniform. The $N = n$ points where $\nu = 1/n$ were placed at random locations in A . Because the resulting time data was highly dependent on point placement, it was extremely noisy. Thus, we did ten runs for each N and took the median. We started with $N = 128$, increasing by eights up to to $N = 192$, for a total of 100 tests. The results are shown in the right-hand columns of Table 5(b). See the right side of Table 6 for scaling equations with respect to N .

5.4.3. *Scaling interaction of W and N on the plane.* Increasing N means one must consider the scaling behavior of the boundary method with respect to N , as described in Section 5.4.2, above. However, there is another relevant limiting factor for large N : the decreasing area size $\mu(A_i) = n^{-1}$ runs up against the accuracy of the reconstruction. For the problem shown in Figure 10, the area of each region is 5.0×10^{-3} . When $w_* = 2^{-11}$, the maximum error for the area of the partition regions is 8.34×10^{-4} . This is 16.7%, about one-sixth of the size of each region.

FIGURE 10. Partitioning with large N

If all we desire is the Wasserstein distance or the boundary set, this error need not be a concern. However, if we want an accurate set of shifts, large N requires that we increase W to match. Hence, we wanted to consider what happens as W and N increase in tandem.

As it turns out, the scaling we observe is consistent with the product of the two scaling behaviors already determined: $\mathcal{O}(WN \log W \log N)$ with respect to time, and $\mathcal{O}(WN^{1/2})$ with respect to storage. See Table 7 for approximate equations.

TABLE 7. Time and storage scaling with respect to both W and N

Time	$T(N, W) \approx 2.853 \times 10^{-6} WN \ln W \ln N$
Storage	$S(N, W) \approx 1.538 \times 10^{-3} WN^{1/2}$

5.4.4. *Scaling in three dimensions and extrapolation to \mathbb{R}^d .* The computations described above can be repeated in three dimensions. We scale W separately by taking a projection of Example 2.2 into the center of the cube $[0, 1]^3$. Then we consider the median of tests when $W = 2^7$ and N ranges from 8 to 80. Finally, we scale W and N together, and consider their combined behavior. Approximate scaling equations are given in Table 8.

TABLE 8. 3-D scaling with respect to W and N

W alone	Time	$T(W) \approx 6.878 \times 10^{-5} W^2 \ln W$
	Storage	$S(W) \approx 2.341 \times 10^{-2} W^2$
N alone	Time	$T(N) \approx 2.849 \times 10^{-1} N \ln N$
	Storage	$S(N) \approx 2.315 \times 10^2 N^{1/3}$
W and N	Time	$T(N, W) \approx 3.531 \times 10^{-6} W^2 N \ln W \ln N$
	Storage	$S(N, W) \approx 1.397 \times 10^{-1} W^2 N^{1/3}$

Taking the combined scaling equations for two and three dimensions, and extrapolating to arbitrary dimension $d \geq 2$, we anticipate scaling of

$$T(d, N, W) \sim \mathcal{O}(W^{d-1} N \log W \log N) \quad \text{and} \quad S(d, N, W) \sim \mathcal{O}(W^{d-1} N^{1/d}).$$

6. CONCLUSIONS AND FUTURE WORK

In this work, we presented the *boundary method*, a new technique for approximating solutions to semi-discrete optimal transportation problems. We gave an algorithmic description and mathematical justification. As we showed, by tackling only the boundary of the regions to be transported, the method has very favorable scaling properties. Under the assumption that all computations are exact, we gave sharp convergence results and presented several examples to highlight performance of the method. We showed that accurate approximations of the partition regions and the Wasserstein distance can be obtained for a multitude of cost functions. Our future work will consider applications of the boundary method to fully continuous mass transportation problems, and consider the impact of estimated computations on convergence.

REFERENCES

- [1] John W. Barrett and Leonid Prigozhin. A mixed formulation of the Monge-Kantorovich equations. *ESAIM: M2AN*, 41:1041–1060, 2007.
- [2] Jean-David Benamou, Guillaume Carlier, Marco Cuturi, Luca Nenna, and Gabriel Peyré. Iterative Bregman projections for regularized transportation problems. *SIAM Journal on Scientific Computing*, 37(2):A1111–A1138, 2015.
- [3] Dimitri P. Bertsekas. *Network Optimization: Continuous and Discrete Models*. Athena Scientific, Belmont, Massachusetts, 1998. <http://web.mit.edu/dimitrib/www/books.htm>. Accessed: 2016-09-16.
- [4] Dimitri P. Bertsekas and David A. Castañón. A generic auction algorithm for the minimum cost network flow problem. *Comput. Optim. Appl.*, 2:229–260, 1993.
- [5] Guy Bouchitté, Giuseppe Buttazzo, and Pierre Seppecher. Shape optimization solutions via Monge-Kantorovich equation. *Comptes Rendus de l’Académie des Sciences – Series I – Mathematics*, 324:1185–1191, 1997.
- [6] Eric A. Carlen and Wilfrid Gangbo. Solution of a model Boltzmann equation via steepest descent in the 2-Wasserstein metric. *Archive for Rational Mechanics and Analysis*, 172:21–64, 2004.
- [7] Guillaume Carlier. A general existence result for the principal-agent problem with adverse selection. *Journal of Mathematical Economics*, 35:129–150, 2001.
- [8] Pierre-Andre Chiappori, Robert McCann, and Brendan Pass. Multi- to one-dimensional optimal transport. To appear in *Comm. Pure Appl. Math*, 2016.
- [9] Marco Cuturi. Sinkhorn distances: Lightspeed computation of optimal transport. In *Advances in Neural Information Processing Systems*, volume 26, pages 2292–2300. Curran Associates, Inc., 2013.
- [10] Xavier Dupuis. The semi-discrete principal agent problem. Presented at “Computational Optimal Transportation” workshop, July 18–22, 2016. <http://www.crm.umontreal.ca/2016/Optimal16/pdf/dupuis.pdf>.
- [11] Brittany D. Froese and Adam M. Oberman. Convergent finite difference solvers for viscosity solutions of the elliptic Monge-Ampère equation in dimensions two and higher. *Journal of Computational Physics*, 260:107–126, 2014.
- [12] Wilfrid Gangbo and Robert J. McCann. The geometry of optimal transportation. *Acta Mathematica*, 177(2):113–161, 1996.
- [13] Steven Haker and Allen Tannenbaum. Optimal mass transport and image registration. In *IEEE Workshop on Variational and Level Set Methods in Computer Vision: Proceedings: 13 July, 2001, Vancouver, Canada*, pages 29–36, Los Alamitos, California, 2001. IEEE Computer Society.
- [14] Richard Jordan, David Kinderlehrer, and Felix Otto. The variational formulation of the Fokker-Planck equation. *SIAM Journal on Mathematical Analysis*, 29(1):1–17, 1998.
- [15] Leonid V. Kantorovich. On the translocation of masses. *C.R. (Doklady) Acad. Sci. URSS (N.S.)*, 37:199–201, 1942.
- [16] Leonid V. Kantorovich. On a problem of Monge. *Uspekhi Mat. Nauk*, 3:225–226, 1948.
- [17] Péter Kovács. Minimum-cost flow algorithms: an experimental evaluation. Technical report, The Egerváry Research Group, 2015.
- [18] Wuchen Li, Stanley Osher, and Wilfrid Gangbo. Fast algorithms for Earth Mover’s distance based on optimal transport and l_1 type regularization i. Preprint, 2016.
- [19] Xi-Nan Ma, Neil S. Trudinger, and Xu-Jia Wang. Regularity of potential functions of the optimal transportation function. *Arch. Ration. Mech. Anal.*, 177(2):151–183, 2005.
- [20] Gaspard Monge. Mémoire sur la théorie des déblais et des remblais. In *Histoire de l’Académie Royale des Sciences de Paris, avec les Mémoires de Mathématique et de Physique pour la même année*, pages 666–704. Académie des sciences (France)., 1781. In French.
- [21] Michael Muskulus, Annelies M. Slats, Peter J. Sterk, and Sjoerd Verduyn-Lunel. Fluctuations and determinism of respiratory impedance in asthma and chronic obstructive pulmonary disease. *Journal of Applied Physiology*, 109:1582–1591, 2010.
- [22] James B. Orlin. Max flows in $\mathcal{O}(nm)$ time, or better. In *Proceedings of the Forty-fifth Annual ACM Symposium on Theory of Computing*, STOC ’13, pages 765–774, New York, NY, USA, 2013. ACM.
- [23] Svetlozar Rachev and Ludger Rüschendorf. *Mass Transportation Problems. Vol I: Theory, Vol II: Applications*. Probability and its applications. Springer-Verlag, New York, 1998.
- [24] Ludger Rüschendorf. Monge-Kantorovich transportation problem and optimal couplings. *Jahresbericht der Deutschen Mathematiker-Vereinigung*, 109(3):113–137, 2007.
- [25] Ludger Rüschendorf and Ludger Uckelmann. Numerical and analytical results for the transportation problem of Monge-Kantorovich. *Metrika*, 51(3):245–258, 2000.

- [26] J.D. Walsh III. The AUCTION ALGORITHMS IN C++ project. Computer software, <http://gatech.jdwalsh03.com/coding.html>.
- [27] J.D. Walsh III and Luca Dieci. General auction method for real-valued optimal transport. Preprint, <http://gatech.jdwalsh03.com/index.html>, 2016.

SCHOOL OF MATHEMATICS, GEORGIA TECH, ATLANTA, GA 30332 U.S.A., TEL.: +1 404-894-9209 FAX: +1 404-894-4409
E-mail address: dieci@math.gatech.edu

SCHOOL OF MATHEMATICS, GEORGIA TECHN, ATLANTA, GA 30332 U.S.A., TEL.: +1 404-894-4401 FAX: +1 404-894-4409
E-mail address: jdwalsh03@gatech.edu